https://doi.org/10.5194/egusphere-2024-3121
Preprint. Discussion started: 8 November 2024

Influence of atmospheric variations in the polar stratosphere of the southern hemisphere during 2002-2022 on polar planetary wave activity

Liang Tang[1], Sheng-Yang Gu[2*], Xiankang Dou[2]

[1] School of Optoelectronic Engineering, Chongqing University of Posts and Telecommunications, Chongqing, China.

[2] Electronic Information School, Wuhan University, Wuhan, China.

*Corresponding author: Sheng-Yang Gu, (gushengyang@whu.edu.cn)

https://doi.org/10.5194/egusphere-2024-3121
Preprint. Discussion started: 8 November 2024

Abstract. Atmospheric planetary waves has long been studied, focusing on the equator and the middle and low latitudes. However, variation of polar planetary wave activity, especially temperature, temporal, and interannual variations of polar planetary waves, remain largely unexplored. In this study, we use MERRA-2 dataset to investigate the impact of atmospheric variations on polar planetary waves there during austral winter from 2002 to 2022. The temperature amplitude and wave periods of each polar planetary wave event were determined using 2-D least-squares fitting. Our results show that, as the zonal wavenumber increases, E1, E2, E3, and E4 occur earlier with weaker peak amplitudes and shorter wave periods. The phase velocities of E1, E2, E3 and E4 are similar to ~40 m/s in the polar atmosphere. In order to elucidate the variations in the observed polar planetary waves and its possible propagation and amplification mechanism, we carry out the diagnostic analyses with MERRA-2 reanalysis data from the surface up to ~ 80 km. Results indicate that the polar planetary waves can be amplified in instability of the mesosphere ~50–60°S and the stratosphere ~70–80°S. The mean flow instability of the strong polar planetary wave during the austral winter mesosphere is greater than that of the weak wave. The selective generation, propagation, and amplification of planetary waves with varying zonal wavenumbers due to variations in background zonal winds in the polar atmosphere. The temperature amplitude of polar planetary wave correlates with solar activity F10.7. The correlation between zonal wavenumber, wave period, and phase velocity implies that polar planetary waves propagate as fixed-phase wave packets.

https://doi.org/10.5194/egusphere-2024-3121
Preprint. Discussion started: 8 November 2024

These results can suggest that, the background atmospheric conditions in the polar regions play a crucial role in modulating the generation, propagation, and amplification of planetary waves. Overall, we analyze their dynamics variation of eastward planetary waves in the polar atmosphere during the 2002-2022 austral winter periods and statistically analyze the interannual variation.

https://doi.org/10.5194/egusphere-2024-3121
Preprint. Discussion started: 8 November 2024

1 Introduction

The winter stratosphere is primarily influenced by dominant large-scale planetary waves, with their interaction with the zonal mean flow serving as the main driving force for winter stratospheric dynamics. Planetary wave activity significantly influences the polar stratosphere thermal and dynamic structure, causing significant changes in wind, temperature, and composition. They also influence the horizontal transport and distribution of substances such as O3, H2O, and CH4 (Coy et al., 2003; Manney et al., 1998; Allen et al., 1997). Recent studies have specifically examined the significant eastward-propagating planetary waves with periods of approximately 2 and 4 days in the polar stratosphere and mesosphere (Tang et al., 2021; Rhodes et al., 2021; Lu et al., 2017; Lu et al., 2013; Alexander and Shepherd, 2010; Watanabe et al., 2009; Tunbridge and Mitchell, 2009; Sandford et al., 2008; Pancheva et al., 2008; Baumgaertner et al., 2008; Merzlyakov and Pancheva, 2007). Two types of zonal mean flow instabilities have been proposed as the sources of these planetary waves: the barotropic instability of the stratospheric polar night jet (polar night jet) and the barotropic/baroclinic instability of the double-jet structure (subtropical mesospheric jet). The winter polar night jet consists of strong eastward zonal winds centered ~50°S–60°S in the upper stratosphere, while the subtropical mesosphere jet is typically located at ~30°S between ~50 and ~70 km.

https://doi.org/10.5194/egusphere-2024-3121
Preprint. Discussion started: 8 November 2024

The polar planetary waves with zonal wavenumbers -1 (E1), -2 (E2), -3 (E3), and -4 (E4) correspond to ~4, ~2, ~1.3, and ~1-day waves respectively. These waves can induce significant changes in wind and temperature in the polar stratosphere and mesosphere (Merzlyakov and Pancheva, 2007; Manney et al., 1998; Lawrence et al., 1995; Manney and Randel, 1993; Fraser et al., 1993; Venne and Stanford, 1979). They analyzed data from the Arctic Esrange (68°N, 21°E) meteor radar and the Microwave Limb Sounder (MLS) instrument on the EOS Aura satellite to investigate polar waves in the winter stratosphere, mesosphere, and lower thermosphere (Sandford et al., 2008). The E2 reaches maximum at the stratopause and may be generated by instability in the polar night jet. They believed that planetary waves are crucial for dynamically coupling different atmospheric layers and influencing ionospheric variability in polar atmosphere.

They employed a middle atmosphere General Circulation Model (GCM) to simulate the characteristics of the E1 (~4-day) wave in the Antarctic winter mesosphere (Watanabe et al., 2009). They found that the eastward forcing from the E1 wave occurred within the double-jet structure, counteracting a portion of the westward forcing from gravity waves. This phenomenon contributes to stabilizing the mean airflow structure of the Antarctic winter mesosphere. They investigated atmospheric diurnal variability with periods ranging from 1.5 to 5 days using neutral meridional

https://doi.org/10.5194/egusphere-2024-3121
Preprint. Discussion started: 8 November 2024

wind data from Esrange meteor radar, as well as atmospheric temperature and pressure data from SABER (Merzlyakov and Pancheva, 2007). Their findings showed that the Eliassen-Palm (EP) fluxes of waves from jet instability are predominantly directed downward. This suggests that dynamic influences from the mesosphere may impact the lower atmosphere. They observed that the eastward propagating planetary waves were predominantly confined to high latitudes during winter (Lu et al., 2013). This limitation could be attributed to the evanescent wave characteristics resulting from a negative refractive index of ~45°S in the equatoria, thereby impeding their propagation towards lower latitudes. They investigated the seasonal variation of eastward E2 in 2007 using temperature and wind data from the Whole Atmosphere Community Climate Model + Data Assimilation Research Testbed (WACCM + DART) (Gu et al., 2017). Their findings showed that E2 mainly occurs in winter, with peak amplitudes in the stratosphere. Temperature amplitude, zonal wind, and meridional wind in southern winters can reach amplitudes of ~10 K, ~20 m/s, and ~30 m/s respectively. Conversely, in northern winters, E2 exhibit only one-third of this strength in temperature amplitude compared to their southern counterparts. They employed WACCM simulations to investigate eastward planetary waves during a significant sudden stratospheric warming (SSW) event occurring in January 2009 within boreal (Rhodes et al., 2021). They believed that planetary and gravity

https://doi.org/10.5194/egusphere-2024-3121
Preprint. Discussion started: 8 November 2024

waves caused eastward wind maxima in the stratosphere and mesosphere before the SSW in the stratosphere. This dual-maxima wind configuration promotes the planetary wave growth through over-reflection due to wind shear instability. They investigated the global variation of eastward propagating wavenumbers E1, E2, E3, and E4 planetary waves in the polar atmosphere using temperature and wind data from the 2019 Modern-Era Retrospective Research Analysis for Research and Applications (MERRA-2) (Tang et al., 2021). Their findings revealed a slightly larger maximum amplitude in the southern hemisphere compared to the northern hemisphere. They observed that as the wavenumber increases, polar planetary wave peak at lower latitudes with smaller amplitudes. Additionally, diagnostic analysis suggested that mean flow instability in the upper stratosphere and upper mesosphere may contribute to enhanced polar planetary waves.

The interannual variation of polar planetary waves in the polar atmosphere lacks comprehensive research. We analyzed polar planetary waves E1, E2, E3, and E4 during austral winter using MERRA-2 data from 2002 to 2022. Section 2 summarizes the MERRA-2 data and analysis methods used in this work. Focusing specifically on occurrence dates, peak amplitudes, and wave periods for each respective event (Sections 3.1 through 3.4). Comparison of E1, E2, E3, and E4 (Section 3.5). In Section 4, we discuss the variations in temperature amplitude, temporal, and

https://doi.org/10.5194/egusphere-2024-3121
Preprint. Discussion started: 8 November 2024

interannual of polar planetary waves and their dynamics. Section 5 provides the summary.

2 Data and Analysis

The air temperature, potential temperature, zonal wind, meridional wind, vertical wind, air density, and model mid-layer height output were obtained from the MERRA-2 dataset with a 3-hourly temporal resolution and a horizontal resolution of 0.5°×0.625°. Recently upgraded using the Goddard Earth Observing System Model Version 5 (GEOS-5) data assimilation system (Gelaro et al., 2017; Molod et al., 2014; Molod et al., 2012), this dataset provides information from 72 different model levels above the surface, with particular focus on levels ranging from 9 to 15. The pressure at the topmost level of the model is set at 0.01 hPa. MERRA-2 has been extensively utilized in various studies investigating phenomena such as planetary waves in polar atmospheres, global thermal tides, climate variability, aerosol and ozone trends and processes (Zamora et al., 2022; Bahramvash Shams et al., 2022; Tang et al., 2021; Ukhov et al., 2020; Bali et al., 2019; Lu et al., 2013). Numerous recent studies have demonstrated that utilizing MERRA-2 data is feasible for our present study.

Time windows of 10, 6, 4, and 4 days were selected to analyze planetary waves E1, E2, E3, and E4 using the least-squares method to obtain fluctuation information for each window. Subsequently, characteristic properties of the planetary waves, such as peak amplitude,

https://doi.org/10.5194/egusphere-2024-3121
Preprint. Discussion started: 8 November 2024

wave period, and occurrence date, were determined (Tang et al., 2021). This approach has proven successful in identifying planetary waves from satellite measurements and reanalysis data (Tang et al., 2021; Gu et al., 2021).

$$y = A\cos[2\pi(\sigma \cdot t + s \cdot \lambda)] + B\sin[2\pi(\sigma \cdot t + s \cdot \lambda)] + C \qquad (1)$$

The values of A, B, and C in Equation (1) were obtained by least-squares fitting. The values of A, B, and C in Formula (1) were obtained by least-square fitting. The frequency and zonal wavenumber are represented by σ and s. The longitude of the satellite samples and UT time are defined by λ and t. Planetary wave amplitude R can be expressed by $R = \sqrt{A^2 + B^2}$.

The baroclinic/barotropic instability in the atmospheric structure arises from the simultaneous equalization of the negative latitude gradient and quasi-geostrophic potential vorticity. The angular speed of the Earth's rotation (Ω), latitude (φ), zonal mean zonal wind ($\bar{u}$), Earth radius (a), air density (ρ), Coriolis parameter (f), buoyancy frequency (N), subscripts vertical (z) and latitudinal (φ) gradients are denoted as in Equation (2).

$$\overline{q_\varphi} = 2\Omega\cos\varphi - \left(\frac{(\bar{u}\cos\varphi)_\varphi}{a\cos\varphi}\right)_\varphi - \frac{a}{\rho}\left(\frac{f^2}{N^2}\rho\bar{u}_z\right)_z \qquad (2)$$

The Eliassen-Palm (EP) flux vectors (F) can be used to calculate the properties of planetary wave propagation (Equation 3). The planetary wave perturbations in the zonal and meridional wind are represented by u' and v', respectively; θ' represents the potential temperature, while w'

https://doi.org/10.5194/egusphere-2024-3121
Preprint. Discussion started: 8 November 2024

represents the vertical wind.

$$\mathrm{F} = \rho a \cos\varphi \begin{bmatrix} \frac{\bar{u}_z \overline{v'\theta'}}{\bar{\theta}_z} - \overline{v'u'} \\ \left[f - \frac{(\bar{u}\cos\varphi)_\varphi}{a\cos\varphi}\right]\frac{\overline{v'\theta'}}{\bar{\theta}_z} - \overline{w'u'} \end{bmatrix} \tag{3}$$

The propagation of planetary waves is favorable only when the square of the refractive index m^2 is positive. The refractive index squared serves as the waveguide for planetary waves, where s represents the zonal wavenumber, c denotes the phase speed, and H stands for the scale height. The equatorial linear velocity, denoted as v_0, T is related to the wave period.

$$m^2 = \frac{\bar{q}_\varphi}{a(\bar{u}-c)} - \frac{s^2}{(a\cos\varphi)^2} - \frac{f^2}{4N^2H^2} \tag{4}$$

$$\mathrm{c} = -v_0 \cos\left(\frac{\varphi\pi}{180}\right)/sT \tag{5}$$

3 Results

Figure 1 illustrates the temporal variations of polar planetary waves E1, E2, E3, and E4 observed during the 2002 austral winter. Figures 1a-1d illustrate the variations of polar planetary waves at different latitudes. The observations show E1 at ~70-80°S and ~50 km, E2 at ~60-70°S and ~50 km, E3 at ~60-70°S km and ~50 km, and E4 at ~50-60°S km and ~50 km. The largest peak of E1 occurs on days 202–212 (~3.125 day/~75 hr, ~7 K), while the other three peaks occur on days 154–164 (~3.75 day/~90 hr, ~4 K), 184–194 (~3.46 day/~83 hr, ~4 K), and 260–270 (~6.5 day/156 hr, ~6 K). The maximum peak of E2 occurs on days 186–192 (~32 hr, ~4 K), with smaller peaks on days 198–204 (~48 hr, ~3 K) and days 208–214

https://doi.org/10.5194/egusphere-2024-3121
Preprint. Discussion started: 8 November 2024

(~38 hr, ~3.5 K). E3 exhibits two peaks, with the strongest occurring on days 154-158 (~26 hr, ~3 K) and a secondary peak on days 186-190 (~22 hr, ~2 K). Additionally, E4 occurs three times: on days 154–158 (~21 hr, ~1.5 K), 192-196 (~29 hr, ~1 K), and 224-226 (~27 hr, ~1 K). The strongest amplitudes for E1, E2, E3, and E4 occur during days 202-212, 186-192, 154-158, and 154 -158 respectively. As the zonal wavenumber increases for polar planetary waves, both wave period and peak amplitude decrease.

We presented the analysis results only for 2002 due to the representative of the wave activities for the entire range of 2002–2022. We thoroughly examined the wavenumber-period spectra for each event to ensure accuracy and validate our findings. Subsequently, we statistically constrained their occurrence date, wave period, and peak amplitude during 2002-2022. The temperature amplitude and wave periods of each event were determined using 2-D least-squares fitting.

3.1 E1

Table 1 lists the 107 E1 events, occurring at ~70–80°S and ~50 km during the austral winter from 2002 to 2022. The E1 appeared earliest on days 142-152 in 2005, 2006, 2009, 2010, and 2021, while latest on days 258-268 in 2011, 2015, and 2018. The shortest wave period observed for E1 was ~53 hr between days 190-200 in 2012, while the longest was ~171 hr between days 242-252 in 2015. E1 shows the smallest peak amplitude

https://doi.org/10.5194/egusphere-2024-3121
Preprint. Discussion started: 8 November 2024

(~4-4.5 K) on days 160-170 in 2003, 158-168 in 2010, and 142-152 in 2021. The largest peak amplitude of E1 reached ~13.5-14 K between days 214-224 in 2003 and 194-204 in 2017. The scatter diagram in Figure 2 shows E1 variations in date-amplitude, period-amplitude, and date-period for the austral winter from 2002-2022. Larger E1 events occur in the middle of the austral winter, while smaller ones occur in the early and late. E1 events with temperature amplitudes exceeding ~8 K mainly occur within ~72-120 hr, while those lasting longer than ~144 hr have stronger temperature amplitudes but lower frequency. The E1 events with longer periods mainly occur in early austral winter, while those with shorter periods tend to happen later. Most temperature amplitudes associated with E1 events surpass ~5 K (Figures 2a, 2d, and 2g).

The histogram shows the distribution of E1 information (Figures 2b, 2e, and 2h). E1 was more frequent at 200-220 days (24 times) and less so at 140-160 days (17 times) and 240-260 days (11 times). E1 events were recorded 60 times between days 180–240, accounting for ~56% of the total. The wave period of E1 is distributed between ~48 and ~192 hr, with 84 times occurring between ~72 and ~120 hr, accounting for ~78.5% of the total, among which 49 times occur between ~72 and ~96 hr. Longer wave periods for E1 are scattered between ~120-192 hr (11 times). The wave period of E1 decreases from ~96 hr on days ~160 to ~70 hr on days ~200. The mean amplitude of E1 is smallest at 140-160 days (~6.5 K), reaching

https://doi.org/10.5194/egusphere-2024-3121
Preprint. Discussion started: 8 November 2024

~8 K at 160-240 days and ~7.5 K at 240-260 days. The mean amplitude of the E1 wave period is larger than ~8 K within ~72-192 hr, with the minimum amplitude occurring within ~48-72 hr (~7 K). The largest mean amplitude of E1 occurs at ~180 days and ~96 hr, followed by a gradual increase at ~72 hr and ~120 hr at ~200 days, exhibiting a distinct branching structure (Figures 2c, 2f, and 2i).

3.2 E2

Table 2 lists the dates, periods, and amplitudes of E2 polar planetary wave events at ~60-70°S and ~50 km during austral winters from 2002 to 2022. The table records 99 E2 events. The E2 appeared earliest on days 142-148 in 2003, 2017, and 2022, while latest on days 256-262 in 2005 and 2011. The shortest wave period of E2 is ~30 hr during days 214-220 and 238-244 in 2017. The longest period of ~58 hr occur on days 256-262 in 2011 and 176-182 in 2012 for E2. The amplitude of E2 was smallest at ~2.5 K on days 246-252 in 2017, and reached the largest amplitude of ~11 K during 174-180 days in 2007 and 220-226 in 2020. Larger E2 events occur in the middle of the austral winter, while smaller ones happen in the early and late. E2 events with temperature amplitudes greater than ~6 K mainly occur in ~38-48 hr, while those other periods have weak temperature amplitudes. The E2 period is shorter in the middle of the austral winter but becomes longer in the early and late. Most E2 events exhibit temperature amplitudes exceeding ~4 K (Figures 3a, 3d, and 3g).

https://doi.org/10.5194/egusphere-2024-3121
Preprint. Discussion started: 8 November 2024

The histogram shows the distribution of E2 information (Figures 3b, 3e, and 3h). E2 events were more frequent (23 times) between 160-180 days, but less so during 140-160 days (13 times) and 240-260 days (14 times). 57 E2 events were recorded between days 160 and 220, accounting for ~57.6% of all total. The wave period distribution from ~28-58 hr for E2. Within ~38-48 hr, 69 E2 events occurred, representing about 69.7% of all total. E2 peaks occurred 37 times between ~43-48 hr. The long-period events for E2 occur between ~53-58 hr (5 times), while the short-period events occur between ~28-33 hr (4 times). The wave period of E2 decreases from ~43 hr at day 160 to ~38 hr at day 200 and then increases to over 43 hr by day 240. The mean amplitude of E2 is ~6.5 K between days 160-240, with minimum amplitudes ~5 K observed on days 140-160 and 240-260. The mean amplitude of the E2 exceeds ~6 K within ~33-58 hr, while the minimum amplitude occurs at ~5 K between ~28-33 hr. The mean amplitude of E2 peaks at ~160 days (~43 hr), ~200 days (~33 hr), and 240 days (~38 hr), accompanied by noticeable branches (Figures 3c, 3f, and 3i).

3.3 E3

Table 3 lists the dates, periods, and amplitudes of the E3 polar planetary waves event at ~60-70°S and ~50 km during austral winters from 2002 to 2022. There were 74 E3 events, with the earliest occurring on days 142-146 in 2022 and the latest on days 260-264 in 2009 and 2018. The shortest wave period for E3 was ~21 hr between days 204-208 in 2006,

https://doi.org/10.5194/egusphere-2024-3121
Preprint. Discussion started: 8 November 2024

while the longest wave period of ~42 hr occurred between days 214-218 in 2019. The peak temperature amplitude of E3 was smallest, ~2-2.5 K on days 156-160 in 2004, 258-262 in 2006, 260-264 in 2009, and 258-262 in 2015. The largest temperature amplitude of E3 reached ~9 K on days 180-184 in 2008. Larger E3 events mainly occur in early austral winter, while smaller ones are more commonly observed in late austral winter. The amplitude of E3 gradually increased from days 140-180, peaked at ~7 K on days 160-180, and then decreased gradually from days 180-260. The E3 temperature amplitude exceeds ~5 K within ~24-32 hr, but weakens and occurs less frequently when the E3 event period exceeds ~32 hr. The E3 exhibits shorter periods in the middle of the austral winter and longer periods in the early and late (Figures 4a, 4d, and 4g).

The histogram illustrates the distribution of E3 information (Figures 4b, 4e, and 4h). The E3 events are most frequent (15 times) between days 160-180, less so (10 times) between days 220-240, and least frequent (9 times) on days 240-260. A total of 43 E3 events occurred between days 140-200, accounting for ~58%. The wave period of E3 from ~20 to ~44 hr, with the majority (60 times) occurring between ~24 and ~32 hr, accounting for ~81.1% of all E3 events. The peak frequency of E3 events is at ~24-28 hr (31 times), followed by ~28-32 hr (29 times). The long-period E3 event occurs four times in ~36-44 hr. The wave period of E3 remains relatively stable at ~29 hr from days 140 to 160. The E3 wave period decreases to

https://doi.org/10.5194/egusphere-2024-3121
Preprint. Discussion started: 8 November 2024

~26 hr from days 180 to 200 and then gradually increases after day 200. The mean amplitude of E3 is ~6 K between days 160 and 200, reaching a minimum of ~3.5 K between days 240 and 260. The E3 wave period typically exceeds ~4 K within ~24-36 hr, with the smallest amplitude occurring at ~20-24 and ~40-44 hr (~3 K). The mean amplitude of E3 peaks was ~6 K on day 160 (~28 hr), ~7 K on day 180 (~24 hr), and ~5 K on day 220 (~28 hr) (Figures 4c, 4f, and 4i).

3.4 E4

The dates, periods, and amplitudes of E4 polar planetary wave events at ~50–60°S and ~50 km during the austral winter period from 2002 to 2022 are listed in Table 4. The table contains a comprehensive list of sixty-nine E4 events, with the earliest occurring on days 142-146 in 2003, 2008, 2009, 2015, and 2021 and the latest on days 254-260 in 2006. The E4 event had a shortest wave period of ~17 hr on days 208-212 in 2021, and the longest wave period was also ~27 hr, occurring on days 224-228 in 2002, 142-144 in 2015, and 186-190 in 2018. The smallest E4 amplitude was ~1-1.5 K on days 154-158 and 192-196 in 2002, while the largest amplitude reached ~6-6.5 K on days 230-234 in 2008 and 164-168 in 2017. Larger E4 events tend to occur earlier in the austral winter, while smaller ones appear later. E4 events with temperature amplitudes above ~3 K mainly occur between ~20 and ~26 hr. The E4 events show small temperature variations and have low frequencies for periods longer than ~27 hr and

https://doi.org/10.5194/egusphere-2024-3121
Preprint. Discussion started: 8 November 2024

shorter than ~20 hr. The wave period of E4 is shorter in the middle of the austral winter but longer in the early and late. After ~200 days, the wave period of the E4 event increased (Figures 5a, 5d, and 5g).

The E4 histogram shows a high frequency of occurrence (17 times) at 160-180 days, a low frequency of occurrence (8 times) at 220-240 days, and another low frequency (4 times) at 240-260 days. There were 48 E4 events recorded between days 140-200, accounting for ~69.6% of all E4 events. The wave period was from ~16-28 hr, with the higher frequency between ~20-26 hr (54 times), accounting for ~78.3% of all E4 events. Long-period events in E4 are observed between ~26-28 hr (7 times), while short-period ones occur between ~16-18 hr (1 time). The wave period of E4 decreased from days 160 to 180 (~22 to ~20 hr), and then remained relatively stable at ~21 hr from day ~200 (Figures 5b, 5e, and 5h). The mean amplitude of E4 peaks at ~4.5 K between 160-180 days, drops to a minimum (~3 K) at 140-160 and 240-260 days, and reaches a maximum of ~6 K at ~160 days (~26 hr) and ~4 K at ~200 days (~22 hr). The mean amplitude of the wave period for E4 from ~16-28 hr is greater than or equal to ~3 K (Figures 5c, 5f, and 5i).

3.5 Comparison of E1, E2, E3, and E4

To further investigate the amplitude and period variabilities of polar planetary waves (E1, E2, E3, and E4) during the austral winter from 2002 to 2022, we statistically analyze their maximum amplitude, corresponding

https://doi.org/10.5194/egusphere-2024-3121
Preprint. Discussion started: 8 November 2024

wave period, and occurrence date.

The occurrence date of planetary waves is considered to be an important indicator of atmospheric waves (Lu et al., 2019; Liu et al., 2019; Forbes and Zhang, 2015; Liu et al., 2013). Figures 6A1, 6B1, 6C1, and 6D1 illustrate the distribution of event dates for each wave. E1 events are mainly observed during days 200–220 (8 times), with a slightly lower frequency during days 140–160 (1 time), and only 5 times during days 220–240. The E2 event is most frequent between days 160 and 180 (6 times), followed by occurrences on days 220–240 (5 times) and days 180–220 (4 times). There is only one E2 event between days 140 and 160. The majority of E3 events occur between days 140 and 200 (20 times), with only one occurring between days 220 and 240. The largest frequency of E4 events is recorded during days 160-180 (11 times), followed by slightly lower frequencies during both periods 180-200 and 200-220 (each occurring three times). Only 4 times were recorded during days 140-160 and 220-240. These results contrast with those of Tang (2021), which used 2019 MERRA2 data to analyze changes in the behavior of polar planetary waves.

The mean amplitudes of dates for events E1, E2, E3, and E4 are illustrated in Figures 6A2, 6B2, 6C2, and 6D2. The diagrams show that the mean peak temperature amplitude of E1 exceeds ~10 K between 140-240 days, reaching ~12 K from 180-200 days. For E2, the mean peak amplitude

https://doi.org/10.5194/egusphere-2024-3121
Preprint. Discussion started: 8 November 2024

only reaches ~10 K during days 220-240, with its strongest peak surpassing ~8 K between days 160-260. The mean amplitude of E3 generally exceeds ~6 K from day 160 to 200, reaching ~7 K between days 180-200, and dropping to only ~3 K during days 220-240. E4 has a mean peak amplitude exceeding ~4 K from day 140 to 240, reaching ~5.5 K in the period of days 180-200. The temperature amplitude of polar planetary waves decreases as the zonal wavenumber increases, which is consistent with the literature suggesting that the propagation and amplification of polar planetary waves are influenced by the background zonal wind (Tang et al., 2021; Lu et al., 2013; Alexander and Shepherd, 2010; Merzlyakov and Pancheva, 2007).

The distribution of wave periods for polar planetary waves is useful for distinguishing the propagation and amplification characteristics of these waves (Lu et al., 2013; Alexander and Shepherd, 2010; Merzlyakov and Pancheva, 2007; Fraser et al., 1993). Figures 6A3, 6B3, 6C3, and 6D3 depict the distribution of periods for E1, E2, E3, and E4. The wave periods of the 18 E1 events from ~72 to ~168 hr, constituting ~85.7% of the total. Events with periods between ~72-96 hr are more common than those in adjacent periods, while only three E1 events have wave periods of ~48-72 hr, ~120-144 hr, and ~144-168 hr respectively. Out of the eighteen E2 periods, fifteen (85.7%) fall within ~33-48 hr, while three events have wave periods of ~28-32 hr and two events with periods ~48-58 hr respectively. The twenty E3 events have wave periods distributed in two

https://doi.org/10.5194/egusphere-2024-3121
Preprint. Discussion started: 8 November 2024

ranges: ~24-28 hr and ~28-32 hr, each occurring ten times. Among the eighteen strongest E4 events, ~42.9% have a period of ~22-24 hr, while only one event has a period of ~18-20 hr. These results are consistent with previous studies on planetary waves conducted in the polar atmosphere (Tang et al., 2021; Lu et al., 2013).

In Figures 6A4, 6B4, 6C4, and 6D4, the mean peak amplitude of E1 exceeds ~8 K within ~48-168 hr, reaching ~12 K in ~96-120 hr, with the smallest peak amplitude occurring between ~48-72 hr (~8 K). The strongest peak amplitude for E2 is ~48 to ~53 hr, reaching ~9 K, significantly stronger than neighboring intervals. The smallest peak amplitude occurs between ~28 and ~33 hr, reaching ~6 K. Meanwhile, the E2 amplitude reaches or exceeds ~6 K from ~33 to ~58 hr. The mean peak amplitude for E3 remains constant at ~6 K in both time intervals of ~24-28 hr and ~28-32 hr. The peak amplitude for E4 exceeds ~3 K from ~18-28 hr, peaking at ~5 K between ~22-24 hr. Our results also consistent with earlier reports that the wave periods of planetary waves E1, E2, E3, and E4 during the austral winter are primarily concentrated in ~4 days, ~2 days, ~1.3 days, and ~1 day (Lu et al., 2013; Merzlyakov and Pancheva, 2007).

The date-period distributions of E1, E2, E3, and E4 are shown in Figures 6A5, 6B5, 6C5, and 6D5. For E1, there is a gradual shift from predominantly occurring ~96 to ~72 hr before the date-period of 160 to 200 days, followed by a return to ~96 hr after the period exceeds 200 days.

https://doi.org/10.5194/egusphere-2024-3121
Preprint. Discussion started: 8 November 2024

Meanwhile, E2 exhibits a distinct distribution during days 160-220 with period of ~33-43 hr. The distribution of E3 is mainly concentrated within ~24-28 hr between days 140 and 180. Additionally, E4 predominantly occurs within days 140-180, with a stable periodicity of ~18-22 hr. The distribution of dates and periods in Figures 6A6, 6B6, 6C6, and 6D6 indicates a gradual increase in the strongest mean amplitude of E1 from ~96-72 hr at ~160 days to encompassing both ~72 hr and ~144 hr at ~200 days, before returning to the original duration of ~96 hr. E2 exhibits distinct periods of ~48-33 hr at ~160 and ~220 days. The distribution of E3 between 160 and 180 days shows a predominant period concentrated within ~28-24 hr. As for E4, it predominantly occurs within the range of 160-200 days with a focus on periods from ~24-20 hr. The results indicate that, while the variations in the zonal wavenumber lead to a weakening and shortening of the temperature amplitude and wave period of planetary waves in the polar atmosphere, the temporal variations also influence the planetary wave amplitude and wave period, suggesting that these changes are modulated by the background zonal wind (Rhodes et al., 2021; Gu et al., 2021; Lu et al., 2019), especially since Figures 6A5 and 6A6 showed the E1 temperature amplitude variation.

4. Discussion

Based on the above statistical results, we find significant variations in temperature amplitude, temporal, and interannual variability of polar

https://doi.org/10.5194/egusphere-2024-3121
Preprint. Discussion started: 8 November 2024

planetary waves in the polar stratosphere. We will discuss the dynamics of polar planetary waves through diagnostic analysis, studying the effects of mean flow instabilities, background zonal wind, critical layer, EP flux, and positive refractive index to reveal their propagation and amplification mechanism. Simultaneously, we investigate the interannual relationship between temperature amplitude of polar planetary waves and solar activity, and study the variation in phase velocity. We analyze the amplitude variations of the five events with the largest and smallest planetary waves from 2002 to 2022. Based on Figure 6A1, 6B1, 6C1, and 6D1, we examine the temporal variations of planetary waves and select events at different moments (early, middle, and late) for average analysis.

4.1 Amplitude variation of E1, E2, E3 and E4

4.1.1 Large and Small of E1

The background zonal wind and the instability of the polar atmosphere are key factors for the propagation and amplification of planetary waves in the polar atmosphere (Tang et al., 2021; Rhodes et al., 2021; Lu et al., 2019). Tang et al. (2021) investigated the 2019 MEARR2 data for the behavior of polar planetary waves and showed that the temperature amplitude of polar planetary waves is correlated with background zonal winds and instability. Figure 7 illustrates the mean spatial structure of E1 largest and smallest amplitudes (5 events), including polar planetary wave temperature, background zonal wind, positive

https://doi.org/10.5194/egusphere-2024-3121
Preprint. Discussion started: 8 November 2024

refractive index, mean flow instabilities, critical layer, and EP flux. E1 shows a large temperature amplitude of ~12 K at ~70-80°S and ~50 km, with an additional peak of ~6.5 K at ~65 km. Small temperature amplitudes of ~7.5 K and ~6.5 K were also observed at ~60 km and ~65 km, respectively. The mean zonal wind for large E1 speeds is ~90 m/s, while for small E1 speeds is ~80 m/s, both occurring between 40-60°S. The zonal winds of small E1 at ~40-60 km and ~70-80°S were faster than those of large E1. The results indicate that the peak speed of background zonal wind in the mid and high latitudes of the Southern Hemisphere is close to the lower polar atmosphere, which hinders E1 propagation and amplification. Conversely, the weaker lower polar atmosphere zonal wind may favor the propagation and amplification of E1.

Large E1 positive refractive region indices have smoother characteristics than those with small E1 amplitudes, enhancing conditions for planetary wave propagation and amplification. EP fluxes are more likely to propagate during Southern Hemisphere winter and undergo significant amplification due to mean flow instabilities and appropriate background winds in the polar and between ~60 km and ~80 km. The mean flow instabilities and background winds at ~50-60°S and ~50-70 km contribute energy to propagate and amplify the EP flux into the lower atmosphere. The large E1 shows slightly weaker mean flow instabilities and background wind at ~40-60°S and ~60-80 km compared to the small

https://doi.org/10.5194/egusphere-2024-3121
Preprint. Discussion started: 8 November 2024

E1. The wave-mean flow interaction near the critical layer (large: ~95 hr and small: ~112 hr) along the green curve enhances E1. The critical layer absorbs or reflects planetary waves from the lower atmosphere as they propagate downward (Tang and Gu, 2023; Rhodes et al., 2021). The positive index region enclosed by the critical layer further facilitates E1 propagation. The positive refractive index region, stronger instability, and weaker background wind at ~50–60°S and ~60–70 km provide sufficient energy for E1 amplification and propagation (Tang et al., 2021). In addition, the strong instability and weak background wind at ~70–80°S and ~40–60 km provide sufficient energy for upward propagation and amplification of the EP flux (Figure 7d). The weak background winds and strong mean flow instabilities in the low polar atmosphere promote the upward propagation and amplification of EP flux. Similarly, favorable background winds and mean flow instabilities at ~60-80 km in mid-latitudes also facilitate the propagation and amplification of EP fluxes into the lower atmosphere. Both instability and suitable background wind conditions are crucial for determining the propagation and amplification of E1. Additionally, EP fluxes can propagate and amplify to the upper polar, potentially explaining the significant E1 amplitude. Compared to the study of Tang et al. (2021) is that these events are representative based on multi-year average results, where there is more relative influence from background condition such as background zonal winds, instability, critical layers, and positive refractive

https://doi.org/10.5194/egusphere-2024-3121
Preprint. Discussion started: 8 November 2024

index.

4.1.2 Large and Small of E2

Figure 8 illustrates the results of large and small E2. Large E2 shows a large temperature amplitude of ~8.5 K at ~60-70°S and ~50 km, with a secondary peak appearing at ~60 km with a value of ~7.5 K. Small E2 shows temperature amplitude of ~5 K and ~4 K at ~60-70°S, ~50 km, and ~60 km, respectively. The mean zonal wind reaches a maximum of ~90 m/s at ~50-60°S and ~40-60 km for large E2, and measures ~90 m/s for small E2. The mean zonal wind speed is greater in large E2 compared to small E2 at ~60-80°S and ~40-60 km. The weaker background zonal wind confinement in the upper polar atmosphere hinders E2 propagation and amplification. Strong background zonal winds may promote the propagation and amplification of E2. These general results for E2 planetary wave are consistent with past study examining the 2011 Antarctic winter McMurdo (77.8° S, 166.7° E), Antarctica (Lu et al., 2013), where background zonal winds dominate the propagation and amplification of the planetary waves.

The large E2 positive index region in the Southern Hemisphere has smoother features compared to the small E2, which facilitates the propagation and amplification of E2 in the polar atmosphere. It is shows that E2 is more likely to propagate during the Southern Hemisphere winter, and mean flow instabilities in the mid-high latitudes between ~40 and ~80

https://doi.org/10.5194/egusphere-2024-3121
Preprint. Discussion started: 8 November 2024

km significantly amplifies E2. As the EP flux moves towards the lower atmosphere, it eventually propagates towards the equator at ~50 km. E2 is amplified and propagated by wave-mean flow interaction near the critical layer (~48 hr) of the green curve, and promoted by a positive refractive index region. In addition, atmospheric instability and favorable background winds contribute to the energy for the propagation and amplification of the EP flux into the lower atmosphere. Based on the diagnostic analysis of small E2, it is found that E2 gains sufficient energy from strong instability and background wind at ~50–60°S and ~60–70 km. This energy is then amplified and propagated to the lower atmosphere through the critical layer (~42 hr) and positive refractive index (Figure 8h). The atmosphere refractive index affects wave propagation characteristics widely (Yue et al., 2012; Chang et al., 2011; Liu et al., 2004). The background wind at ~40-60°S and ~60-80 km is weaker for large E2 than for small E2, while the instability of large E2 and small E2 at ~50-60°S and ~60-70 km is similar. Our results show that u the planetary waves absorbed sufficient energy for amplification, under the background conditions of large E2. TA similar region of instability (~60-70°S and ~40 km) is also observed in (Watanabe et al., 2009; Manney et al., 1998; Lawrence et al., 1995; Allen et al., 1997), while no associated with significant EP flux.

4.1.3 Large and Small of E3

https://doi.org/10.5194/egusphere-2024-3121
Preprint. Discussion started: 8 November 2024

The large E3 and small E3 are shown in Figure 9. The temperature amplitudes of large E3 reach ~6.5 K at ~60-70°S and ~50 km, with peaks of ~3.5 K and ~3 K at ~60 km and ~70 km, which is consistent with the results of (Tang et al., 2021). Meanwhile, the amplitude of small E3 is ~3.5 K at ~60-70°S and ~50 km, with peak temperatures of ~3 K and ~2.5 K at ~60 km and ~70 km. The zonal wind speed peaks at ~115 m/s (large E3) and ~95 m/s (small E3) between 40-60°S and ~60 km. The mean zonal wind speed of large E3 is greater than that of small E3 at ~40-60°S and ~60-80 km. Strong zonal wind background enhances the propagation and amplification of E3. Meanwhile, the polar background zonal wind of large E3 is weaker than that of small E3. This suggests that E3 propagation in the polar atmosphere is influenced by weaker zonal winds. Consistent with previous studies, E3 is confined to the Southern Hemisphere polar during the austral winter (Lu et al., 2013; Merzlyakov and Pancheva, 2007).

The positive index region of large E3 exhibits smoother characteristics in the propagation area compared to that the small E3, which facilitates the propagation and amplification of E3. These regions are only in the Southern Hemisphere, indicating that E3 is more likely to propagate and amplify in the Southern Hemisphere (Tang et al., 2021; Lu et al., 2013; Fraser et al., 1993). The mean flow instabilities of E3 at ~50-70 km in mid-high latitudes, along with suitable background winds, significantly enhances the propagation of planetary waves. Additionally, the interaction

https://doi.org/10.5194/egusphere-2024-3121
Preprint. Discussion started: 8 November 2024

near the critical layer at ~30 hr and within the positive index region further enhances the E3 propagation. Notably, the weak atmospheric instability and strong background winds of large E3 at ~40-60°S and ~60-80 km, provide sufficient energy for the propagation and amplification of the EP flux into the lower atmosphere, eventually pointing toward the equator at ~50 km (Figure 9d). The EP flux of small E3 is directed towards the lower atmosphere and amplified through interaction at the critical layer (~26 h). In addition, strong instability and weak background winds at ~40–60°S and ~60–80 km provides the energy to enhance E3 propagation (Figure 9h). The EP flux of E3 eventually points to the equator at ~50 km. The stronger the background wind at ~50-60°S and ~60-70 km, the greater the temperature amplitude of E3. We propose that the background winds and instability at the ~50–60°S and ~60–70 km are the primary factors driving the propagation and amplification of EP flux into the lower atmosphere. (Tang et al., 2021; Manney and Randel, 1993) also supports the conclusion that equatorward momentum flux events appear to be consistent with the instability of the double-jet structure.

4.1.4 Large and Small of E4

Figure 10 shows the mean spatial structure of large and small E4. The mean temperature amplitudes of large E4 are ~5 K and ~3.5 K at ~50-60°S, as well as ~50 km and ~70 km. Meanwhile, Small E4 exhibits temperature amplitudes of ~2 K (~50 km) and ~1.5 K (~65 km) at ~50-60°S.

https://doi.org/10.5194/egusphere-2024-3121
Preprint. Discussion started: 8 November 2024

Temperature amplitude measurements during planetary wave activity in the southern polar atmosphere indicate that amplitude decreases with increasing zonal wavenumber (Tang et al., 2021; Lu et al., 2013; Alexander and Shepherd, 2010; Watanabe et al., 2009; Merzlyakov and Pancheva, 2007; Fraser et al., 1993). The mean zonal wind speed of the large E4 reaches ~115 m/s at ~40-50°S, and ~60 km, while the small E4 has a mean zonal wind speed of ~95 m/s at the same latitude and altitude. Additionally, the zonal wind speed of large E4 exceeds that of small E4 at ~40-50°S and ~60 -80 km. A strong background zonal wind promotes the propagation and amplification of E4. The background zonal wind of large E4 is stronger than that of small E4 in the mid-high latitudes. This indicates that strong background zonal winds influence the propagation and amplification of E4 in the polar atmosphere. This is consistent with earlier studies in the polar atmosphere (Merzlyakov and Pancheva, 2007; Venne and Stanford, 1979), indicating that background zonal winds modulate the propagation and amplification of planetary waves. Previous studies of the polar planetary wave E4 have shown that the temperature amplitude and wave period are more similar to tidal waves s compared to others zonal wavenumber (Tang et al., 2021; Lu et al., 2013).

Compared to the small E4, the positive refractive index region of the large E4 exhibits smoother features in the middle atmosphere at mid-latitudes, which facilitates the E4 propagation and amplification. The EP

https://doi.org/10.5194/egusphere-2024-3121
Preprint. Discussion started: 8 November 2024

flux of E4 is similar to that of E3. For E4, in the middle and high latitudes, between ~60 and ~80 km, mean flow instabilities significantly enhances E4. The EP flux of E4 propagating into the lower atmosphere and eventually reaches the equator at ~50 km. The interaction of waves near the critical layer (~23 hr and ~23 hr) amplifies and propagates E4, with the positive refractive index region providing support. The strong instability and strong background winds of the large E4 at ~40-60°S and ~60-80 km provide sufficient energy for the propagation and amplification of the EP flux into the lower atmosphere. In addition, small E4 gains energy under weak instability and weak background wind at ~40-60°S and ~60-80 km, then amplifies and propagates into the lower atmosphere. The background wind at ~40-60°S and ~60-80 km is slightly stronger for large E4 than for small E4, and the instability at ~40-60°S and ~60-80 km is also stronger for large E4 compared to small E4. Large E4 absorbs sufficient energy for amplification under background conditions, as shown in Figure 10a and 10e, resulting in a stronger temperature amplitude, which is consistent with the results of (Lu et al., 2013; Merzlyakov and Pancheva, 2007).

4.2 Temporal variation of E1, E2, E3 and E4

4.2.1 Temporal variation of E1

Based on Figure 6A1, we selected E1 events occurring at 140-160 days (early E1), 200-220 days (mid E1), and 220-240 days (late E1) for average analysis (Figure 11). Consistent with previous studies, polar

https://doi.org/10.5194/egusphere-2024-3121
Preprint. Discussion started: 8 November 2024

planetary waves are limited to high frequencies in certain temporal and low frequencies in others temporal (Tang et al., 2021; Lu et al., 2013; Merzlyakov and Pancheva, 2007). The mean zonal wind reaches a maximum of ~100 m/s at ~30-40°S and ~50-70 km (early E1), while for smaller amplitudes it measures ~90 m/s (mid E1) at ~50-60°S and ~30-40 km, and a maximum of ~95 m/s at~30-40°S and ~50-70 km (late E1). The early E1 mean zonal winds exhibited strong velocities in the upper atmosphere at mid-latitudes. The strongest zonal winds gradually shifted to the lower polar atmosphere, as temporal into the middle and late. Strong background zonal wind in the middle latitudes inhibits E1 propagation and amplification, while weak wind favors it. The positive index region of middle E1 displays smoother features in the Southern Hemisphere compared to the early and late E1, promoting the propagation and amplification of E1 in polar atmosphere.

The results indicate that E1 propagates more easily during the winter in the Southern Hemisphere, and that the mean flow instabilities at mid-high latitudes of ~60 to ~70 km significantly enhances E1. As the two EP fluxes move towards the lower and upper atmosphere. The early, middle, and late E1 waves are amplified and propagated near the mean critical layer of the green curve (~99 hr, ~93 hr, and ~95 hr) through wave-mean flow interaction. The mean critical layer of E1 is close to ~4 days (~96 hr). They are also enhanced in the positive index region. In addition, the mean flow

https://doi.org/10.5194/egusphere-2024-3121
Preprint. Discussion started: 8 November 2024

instabilities and favorable background winds in early, middle, and late E1 provide energy for the propagation and amplification of the EP flux into the lower atmosphere. The middle E1 shows weaker instability compared to early and late E1. The weak background zonal wind of early E1 in the lower polar atmosphere facilitated the propagation of EP flux to the upper atmosphere, while in the middle and late, the strong background zonal wind in the polar hindered this propagation to the upper polar atmosphere. The results indicate that the weak background wind and strong instability at ~40-60°S and ~60-80 km favor the propagation and amplification of E1 to the polar lower atmosphere. The weak background zonal wind and strong instability of the lower atmosphere in the polar provide energy for E1 propagation to the upper atmosphere. The mid E1 shows greater instability in the polar lower atmosphere compared to early and late E1. Our findings suggest that the propagation and amplification of E1 are primarily influenced by the background zonal wind and instability in the polar atmosphere (Pancheva et al., 2008; Manney et al., 1998; Lawrence et al., 1995).

4.2.2 Temporal variation of E2

Based on Figure 6B1, we selected E2 events occurring at 140-160 days (early E2), 160-180 days (mid E2), and 240-260 days (late E2) for average analysis (Figure 12). The mean zonal wind reaches ~125 m/s (early E2) and ~115 m/s (mid E2) in the ~30-40°S and ~60 km, and a maximum

https://doi.org/10.5194/egusphere-2024-3121
Preprint. Discussion started: 8 November 2024

of ~90 m/s at~50-60°S and ~40 km (late E2). The mean zonal wind speed of early E2 is greater than that of mid and late E2, at ~30-40°S and ~60 km. The results indicate that the strong background zonal wind in the upper atmosphere at mid-latitudes supports the E2 propagation and amplification. A weak background zonal wind does not create favorable conditions for E2 propagation and amplification. Early and mid E2 show stronger background zonal winds compared to late E2, suggesting that stronger zonal winds tend to influence E2 propagation in polar atmosphere. The positive refractive index region of the mid E2 has smoother features at mid-latitudes, facilitating the E2 propagation and amplification (Tang et al., 2021; Lu et al., 2013).

For E2, the mean flow instabilities in the mid-high latitudes at ~60-80 km significantly enhances E2. The E2 EP flux propagating into the lower atmosphere and eventually reaches the equator at ~50 km. E2 is amplified and propagated through the interaction of waves near the critical layer (~42 hr, ~47 hr, and ~41 hr), with the positive refractive index region providing support. The mean critical layer for mid E2 is closer to ~2 days (~48 hr). The stronger mean flow instabilities of early E2 at ~40-60°S and ~60-80 km compared to the mid and late. The instability in the upper atmosphere provides sufficient energy for E2 to propagation and amplification in the lower atmosphere. Early E2 strong instability in the mid-latitude upper atmosphere, but is hindered by a strong background zonal wind, which

https://doi.org/10.5194/egusphere-2024-3121
Preprint. Discussion started: 8 November 2024

limits E2 propagation and amplification. Conversely, weak instability of E2 in the mid-latitude is offset by a favorable background zonal wind that promotes propagation and amplification. Late E2 encounters unfavorable conditions for propagation and amplification due to weak background zonal winds. Mid E2 gains energy at ~40-60°S and ~60-80 km under suitable zonal wind conditions, then amplifies and propagates to the lower atmosphere. Our findings indicate that strong background zonal winds and polar instability primarily affect the E2 propagation and amplification, similar to the result by (Alexander and Shepherd, 2010; Tunbridge and Mitchell, 2009; Pancheva et al., 2008)

4.2.3 Temporal variation of E3

Based on Figure 6C1, we selected E3 events occurring at 140-160 days (early E3), 160-180 days (mid E3), and 220-240 days (late E3) for average analysis (Figure 13). The mean zonal wind reaches ~105 m/s (early E3) and ~120 m/s (mid E3) in the ~40-60°S and ~50-60 km. The mean zonal wind speed of late E3 is weaker than that of early and mid E3. The strong background zonal wind creates more favorable conditions for the propagation and amplification of E3 (Lu et al., 2013). This suggests that the propagation and amplification of E3 in polar atmosphere are influenced by strong background zonal wind. The positive index region of mid E3 shows smoother characteristics in the propagation compared to early and late E3, which promotes the propagation and amplification. The speed of the background zonal wind is the primary factor in temporal variation, similar to the result by (Tang et al., 2021; Merzlyakov and Pancheva, 2007).

The mean flow instabilities of E3 at ~50-70 km in mid-high latitudes, along with suitable background winds, significantly enhances the propagation of planetary waves. The interaction near the critical layer at (~30 hr, ~29 hr, and ~24 hr) and within the positive index region further boosts the propagation of E3. The mean critical layer for early and mid E3 is close to ~1.3 days (~31 hr). The atmospheric instability and background winds at ~40-60°S and ~60-80 km provide sufficient energy for the EP flux to propagate and amplify into the lower atmosphere, ultimately directing towards the equator at ~50 km. The instability of mid E3 is weaker than that of late, but stronger than that of early. A stronger background zonal wind of E3 at ~50–60°S and ~60–70 km enhances the propagation and amplification of E3. We believe that the background wind and instability of E3 in the upper atmosphere at mid-high latitudes are the primary drivers of EP flux propagation and amplification in the lower atmosphere (Tang et al., 2021).

4.2.4 Temporal variation of E4

Based on Figure 6D1, we selected E4 events occurring at 140-160 days (early E4), 160-180 days (mid E4), and 220-240 days (late E4) for average analysis (Figure 14). The mean zonal wind speed reaches a maximum of ~115 m/s at ~40-50°S and ~60 km (early E4), increases to

https://doi.org/10.5194/egusphere-2024-3121
Preprint. Discussion started: 8 November 2024

~120 m/s in mid E4, and then drops to ~75 m/s in late E4. The mean zonal wind speed is greater in mid E4 compared to early and late at ~40-60°S and ~60-80 km. The strong background zonal wind facilitates the E4 propagation and amplification. A strong background zonal wind creates more favorable conditions for the propagation and amplification of E4. The positive index regions of mid E4 have smoother features in the Southern Hemisphere compared to the early and late E4 positive index regions, which facilitating the propagation and amplification of E4 in the polar atmosphere (Lu et al., 2013; Merzlyakov and Pancheva, 2007).

The results indicate that E4 is more likely to propagate during the winter in the Southern Hemisphere. The mean flow instabilities at mid-high latitudes of ~60-80 km significantly enhances E4. As the EP flux moves towards the lower atmosphere, it eventually propagates towards the equator at ~50 km. E4 is amplified and amplified near the critical layer (~23 hr, ~23 hr, and ~25 hr) of the green curve through wave-mean flow interaction. The mean critical layer of E4 is close to ~1 day (~24 hr). Atmospheric instability and favorable background winds provide energy for propagation and amplification the EP flux into the lower atmosphere. Through diagnostic analysis, it was discovered that E4 derived sufficient energy from the strong instability and background wind at ~50–60°S and ~60–70 km. Our findings indicate that E4 can absorb sufficient energy to undergo amplification in the strong instability and favorable background

https://doi.org/10.5194/egusphere-2024-3121
Preprint. Discussion started: 8 November 2024

zonal winds, similar to that presented by (Tang et al., 2021).

4.2.5 Variation of critical layer

Figure 15 illustrates the mean structure of the critical layers E1, E2, E3, and E4 during the early and late, and during the high frequency. The characteristics of E1, E2, E3, and E4 critical layers were analyzed within a 10-day window on different occurrence dates. Figure 15a, 15b, and 15c demonstrate the instability, background zonal wind, and critical layer structure of E1 during days 145-155, 205-215, and 245-255. E1, E2, E3, and E4 polar planetary waves have distinct wave periods at the same temporal, while their phase velocities are notably similar (Tang et al., 2021; Lu et al., 2013; Alexander and Shepherd, 2010; Merzlyakov and Pancheva, 2007). Figure 15a exhibits greater instability compared to Figure 15b and 15c. The 4-day critical layer of E1 in Figure 15a and 15b aligns with the edge of instability. In Figure 15c, the critical layer is distant from the instability in the upper atmosphere at mid-latitudes. Cannot supply sufficient energy for the E1 propagation and amplification. The atmospheric background of Figure 15b offers more favorable conditions for E1 propagation and amplification. Simultaneously, the wave-mean interaction near the critical layer of the green curve (~4-day) enhances E1. The absence of critical layer (~2 days/yellow curve, ~1.3 days/cyan curve, and ~1 day/magenta curve) indicates that these wave periods are unsuitable for occurrence, propagation, and amplification.

https://doi.org/10.5194/egusphere-2024-3121
Preprint. Discussion started: 8 November 2024

For E2 (Figure 15d-15f), The mean flow instabilities at ~60°S and ~60 km, which potentially facilitate E2. The amplification of E2 is enhanced by wave-mean interaction near the critical layer of the yellow curve (~2-day). Conversely, no critical layers (~4-day, ~1.3-day, and ~1-day) are found in proximity to the instability region, hindering the occurrence, propagation, and amplification of these wave periods. Weaker background winds and instability also impede E2. For E3 and E4, we observe similar characteristics in their occurrence, propagation, and amplification as those observed for E2 within the atmospheric background on 165-175 days. The wave-mean interaction near the critical layer (~1.3-days/cyan curve and ~1-day/magenta curve) enhances the amplification of E3 and E4 (Figure 15g-15i and Figure 15j-15l). In general, polar planetary waves undergo selective amplification by the background atmosphere during their occurrence, propagation, and amplification processes at different zonal wavenumbers.

4.3 Interannual variation of E1, E2, E3 and E4

To put the interannual variation of polar planetary waves results into perspective, temperature amplitude, solar activity F10.7, and phase velocity data from 2002 to 2022, indicate that variations in polar planetary wave behavior are linked to F10.7, followed by a steady variation in phase velocity over the years. The temperature amplitudes of the E1, E2, E3, and E4 polar planetary waves during austral winter periods from 2002 to 2022

https://doi.org/10.5194/egusphere-2024-3121
Preprint. Discussion started: 8 November 2024

are shown in Figure 16a-16d. The maximum temperature of E1 was ~13-14 K in 2003, 2005, 2010, 2012, and 2017. The temperature amplitude of E1 is equal to or greater than ~10 K in 2002, 2004, 2006, 2009, 2011, 2014, 2015, 2016, 2018, 2021, and 2022. The temperature amplitude during the solar activity minimum years of 2007, 2008, 2013, 2019, and 2020, was only ~4-5 K. The E2 temperature amplitude peaked at ~10-11 K in 2007, 2008, 2020, and 2022. E2 reached ~8-10 K in 2006, 2009, 2011, 2013, 2014, 2015 and 2017. In other years, the temperature amplitude was only ~6-8 K. The temperature amplitude of E3 was strongest in 2008, reaching ~8-9 K, slightly higher than the ~7-8 K in 2003, 2004, 2005, 2007, 2011 and 2016, and less than ~7 K in other years. The E3 during the austral winter period was most pronounced in 2008, reaching amplitudes of ~8-9 K, slightly exceeding those observed in 2003, 2004, 2005, 2007, 2011, and 2016 (~7–8 K). Amplitudes weaker than ~7 K were observed in other years. The strongest temperature amplitude for E4 was in 2008, peaking at ~6-7 K. In 2002, 2007, and 2020, the amplitude of E4 only reached ~1-3 K. In other years, the temperature amplitude was ~3-6 K.

E1 temperature amplitude decreased significantly during solar minima in 2007, 2008, and 2020, while E1 amplitudes increased significantly during the solar maximum years of 2003, 2012, and 2022 compared to adjacent years like 2004, 2013, and 2021. Additionally, we found that E2 amplitude shows a negative correlation with solar activity.

https://doi.org/10.5194/egusphere-2024-3121
Preprint. Discussion started: 8 November 2024

Notably, the exceptionally strong E2 activity in 2006-2009, 2019, and 2020 coincided with solar minimum conditions. Unlike E1, the amplitude of E3 remains relatively constant throughout the solar cycle. Additionally, there are similar variation characteristics between E4 and E1. Temperature amplitude of E1 is positively associated with solar activity. The temperature amplitude of E2 in 2012 was relatively weak due to strong solar activity in 2011 and 2013, indicating a negative correlation. The correlation between the temperature amplitude of E3 and solar activity is weak. The temperature amplitude of E4 is positively correlated with solar activity, but anomalies occurred in 2008 and 2017.

Figure 16e shows the phase velocities of the strongest events (E1-E4) during the austral winter periods from 2002 to 2022. The phase velocity of E1 was ~24 m/s in 2006 and ~58 m/s in 2020, resulting in a difference of 34 m/s between the maximum and minimum phase velocities. The minimum phase velocity of E2 was ~33 m/s in 2012, while the maximum phase velocity reached ~59 m/s in 2002. As for E3, the phase velocity reached ~53 m/s in both 2016 and 2020 (maximum), and only ~36 m/s in 2018 (minimum). The maximum and minimum phase velocities of E4 in 2002 and 2013 were ~35 m/s and ~50 m/s, respectively. The phase velocity change of E1 in 2006 was significant, while the phase velocity changes for E2, E3, and E4 years were relatively stable. The mean phase velocities for E1, E2, E3, and E4 are ~41 m/s, ~46 m/s, ~45 m/s, and ~42 m/s respectively.

https://doi.org/10.5194/egusphere-2024-3121
Preprint. Discussion started: 8 November 2024

We propose that polar planetary waves propagate as fixed-phase wave packets, selectively amplifying planetary waves with different zonal wavenumbers due to variations in the background atmospheres while maintaining similar phase velocities, similar to that presented by (Tang et al., 2021; Lu et al., 2013; Alexander and Shepherd, 2010).

5. Summary

The objective of this study is to analyze the occurrence date, wave period, and peak amplitude distribution of planetary waves E1, E2, E3, and E4 in the stratosphere and mesosphere using the 2002-2022 MERRA2 data on wind and temperature, explore their amplitude and temporal variation, while also investigating their interannual variation. This is motivated by a large inventory of past studies that examined single year variation and related topics (SSWs) but did not have a comprehensive study of the propagation and amplification, which is a gap addressed by this study. An important result in this work is that the propagation and amplification characteristics of polar planetary waves during austral winter periods are influenced by background zonal winds and atmospheric instability, and that there is significant variability temperature amplitude, wave period, and temporal variations examined for a given zonal wavenumber. This point is crucial as it enables us to examine the correlation between polar planetary wave propagation, amplification, and zonal wavenumbers, which have been archived for this (Tang et al., 2021; Lu et al., 2013; Alexander and

https://doi.org/10.5194/egusphere-2024-3121
Preprint. Discussion started: 8 November 2024

Shepherd, 2010; Merzlyakov and Pancheva, 2007) and other planetary waves. The key findings of this study are summarized below:

Peaks of E1, E2, E3, and E4 decrease in amplitude and latitude with increasing wavenumber, while the timing of planetary wave events advances. The wave period and amplitude of E1 is mainly from ~3 to ~5 days and ~12 K, while E2: is ~38 to ~48 hr and ~10 K, E3: ~24 to ~32 hr and ~8 K, E4: ~22 to ~24 hr and ~6 K. The wave periods of E1, E2, and E3 progressively shorten during early to middle austral winter and lengthen during late austral winter. Stratospheric dynamics still significantly influence the propagation and amplification of planetary waves in the polar. Planetary waves are confined to high latitudes due to the negative refractive index at ~45°S in the equatorial direction, which results in their evanescent properties and prevents them from propagating to lower latitudes. EP flux and instability analysis indicate that the baroclinic instability between ~50°S-60°S caused by the stratospheric polar night jet / "double jet" structure is likely responsible for generating these waves.

Polar planetary waves exhibit two EP fluxes: one propagates from the lower to the upper atmosphere, while the other from the upper to the lower atmosphere. EP fluxes ultimately deflect towards the equator at ~50 km. The polar planetary wave amplifies and propagates through suitable background wind and instability in middle and high latitudes. The stronger atmospheric instability and favorable polar background winds promote the

https://doi.org/10.5194/egusphere-2024-3121
Preprint. Discussion started: 8 November 2024

propagation and amplification of planetary waves, consequently leading to greater temperature amplitudes. The background atmosphere selectively amplifies planetary waves during their occurrence, propagation, and amplification at various zonal wavenumbers. The eastward planetary wave propagates in the polar atmosphere as a fixed-phase wave packet. E1, E2, E3, and E4 are selectively amplified by different background atmospheres while maintaining similar phase velocities. The polar planetary wave activity is linked to solar activity, with E1 showing a positive correlation to E4, E2 displaying a negative correlation, and E3 having no strong correlation. Overall, we analyze their dynamics variation of eastward planetary waves in the polar atmosphere during the 2002-2022 austral winter periods and statistically analyze the interannual variation.

It is important to consider some limitations in this study to improve upon in future work, such as a need for more statistical data, a need for more detailed measured data, a lack of measurements relating to the effects of polar particle deposition and strong magnetic fields, and the influence of the unique atmospheric conditions and geographical features of the polar atmosphere on planetary wave structure. This work motivates continued attention to the polar planetary wave behavior and provides a special conclusion to enrich the polar atmospheric research for several decades.

Data availability. MERRA-2 data are available at http://disc.gsfc.nasa.gov.

Code availability. The code is available at https://www.scidb.cn/s/n6nIny.

Author contributions. LT carried out the data processing and analysis and wrote the manuscript. SYG and XKD contributed to reviewing the article.

Competing interests. The authors declare that they have no conflict of interest.

Acknowledgements. This work was performed in the framework of the Space Physics Research (SPR). The authors thank NASA for free online access to the MERRA-2 temperature reanalysis.

Financial support. This research work was supported by the National Natural Science Foundation of China (42374195, 42188101).

https://doi.org/10.5194/egusphere-2024-3121
Preprint. Discussion started: 8 November 2024

References

Alexander, S. P. and Shepherd, M. G.: Planetary wave activity in the polar lower stratosphere, Atmos. Chem. Phys., 10, 707-718, 10.5194/acp-10-707-2010, 2010.

Allen, D. R., Stanford, J. L., Elson, L. S., Fishbein, E. F., Froidevaux, L., and Waters, J. W.: The 4-Day Wave as Observed from the Upper Atmosphere Research Satellite Microwave Limb Sounder, Journal of the Atmospheric Sciences, 54, 420-434, 10.1175/1520-0469(1997)054<0420:TDWAOF>2.0.CO;2, 1997.

Bahramvash Shams, S., Walden, V. P., Hannigan, J. W., Randel, W. J., Petropavlovskikh, I. V., Butler, A. H., and de la Cámara, A.: Analyzing ozone variations and uncertainties at high latitudes during sudden stratospheric warming events using MERRA-2, Atmos. Chem. Phys., 22, 5435-5458, 10.5194/acp-22-5435-2022, 2022.

Bali, K., Dey, S., Ganguly, D., and Smith, K. R.: Space-time variability of ambient PM2.5 diurnal pattern over India from 18-years (2000–2017) of MERRA-2 reanalysis data, Atmos. Chem. Phys. Discuss., 2019, 1-23, 10.5194/acp-2019-731, 2019.

Baumgaertner, A. J. G., McDonald, A. J., Hibbins, R. E., Fritts, D. C., Murphy, D. J., and Vincent, R. A.: Short-period planetary waves in the Antarctic middle atmosphere, Journal of Atmospheric and Solar-Terrestrial Physics, 70, 1336-1350, https://doi.org/10.1016/j.jastp.2008.04.007, 2008.

Chang, L. C., Palo, S. E., and Liu, H.-L.: Short-term variability in the migrating diurnal tide caused by interactions with the quasi 2 day wave, Journal of Geophysical Research: Atmospheres, 116, https://doi.org/10.1029/2010JD014996, 2011.

Coy, L., Štajner, I., DaSilva, A. M., Joiner, J., Rood, R. B., Pawson, S., and Lin, S. J.: High-Frequency Planetary Waves in the Polar Middle Atmosphere as Seen in a Data Assimilation System, Journal of the Atmospheric Sciences, 60, 2975-2992, 10.1175/1520-0469(2003)060<2975:Hpwitp>2.0.Co;2, 2003.

Forbes, J. M. and Zhang, X.: Quasi-10-day wave in the atmosphere, Journal of Geophysical Research: Atmospheres, 120, 11,079-011,089, https://doi.org/10.1002/2015JD023327, 2015.

Fraser, G. J., Hernandez, G., and Smith, R. W.: Eastward-moving 2–4 day waves in the winter Antarctic mesosphere, Geophysical Research Letters, 20, 1547-1550, https://doi.org/10.1029/93GL01707, 1993.

Gelaro, R., McCarty, W., Suárez, M. J., Todling, R., Molod, A., Takacs, L., Randles, C. A., Darmenov, A., Bosilovich, M. G., Reichle, R., Wargan, K., Coy, L., Cullather, R., Draper, C., Akella, S., Buchard, V., Conaty, A., da Silva, A. M., Gu, W., Kim, G.-K., Koster, R., Lucchesi, R., Merkova, D., Nielsen, J. E., Partyka, G., Pawson, S., Putman, W., Rienecker, M., Schubert, S. D., Sienkiewicz, M., and Zhao, B.: The Modern-Era Retrospective Analysis for Research and Applications, Version 2 (MERRA-2), Journal of Climate, 30, 5419-5454, 10.1175/JCLI-D-16-0758.1, 2017.

Gu, S.-Y., Liu, H.-L., Pedatella, N. M., Dou, X., and Liu, Y.: On the wave number 2 eastward propagating quasi 2 day wave at middle and high latitudes, Journal of Geophysical Research: Space Physics, 122, 4489-4499, https://doi.org/10.1002/2016JA023353, 2017.

Gu, S.-Y., Tang, L., Hou, X., Zhao, H., Teng, C.-K.-M., and Dou, X.: Quasi-Two-Day Waves in the Northern Hemisphere Observed by TIMED/SABER Measurements During 2002–2019, Journal of Geophysical Research: Space Physics, 126, e2020JA028877, https://doi.org/10.1029/2020JA028877, 2021.

Lawrence, B. N., Fraser, G. J., Vincent, R. A., and Phillips, A.: The 4-Day Wave in the Antarctic

https://doi.org/10.5194/egusphere-2024-3121
Preprint. Discussion started: 8 November 2024

Mesosphere, J Geophys Res-Atmos, 100, 18899-18908, Doi 10.1029/95jd01168, 1995.

Liu, G., England, S. L., and Janches, D.: Quasi Two-, Three-, and Six-Day Planetary-Scale Wave Oscillations in the Upper Atmosphere Observed by TIMED/SABER Over ~17 Years During 2002–2018, Journal of Geophysical Research: Space Physics, 124, 9462-9474, https://doi.org/10.1029/2019JA026918, 2019.

Liu, H. L., Talaat, E. R., Roble, R. G., Lieberman, R. S., Riggin, D. M., and Yee, J. H.: The 6.5-day wave and its seasonal variability in the middle and upper atmosphere, Journal of Geophysical Research: Atmospheres, 109, https://doi.org/10.1029/2004JD004795, 2004.

Liu, L., Chen, Y., Le, H., Ning, B., Wan, W., Liu, J., and Hu, L.: A case study of postmidnight enhancement in F-layer electron density over Sanya of China, Journal of Geophysical Research: Space Physics, 118, 4640-4648, https://doi.org/10.1002/jgra.50422, 2013.

Lu, X., Chu, X., Chen, C., Nguyen, V., and Smith, A. K.: First Observations of Short-Period Eastward Propagating Planetary Waves From the Stratosphere to the Lower Thermosphere (110 km) in Winter Antarctica, Geophysical Research Letters, 44, 10,744-710,753, https://doi.org/10.1002/2017GL075641, 2017.

Lu, X., Chu, X., Fuller-Rowell, T., Chang, L., Fong, W., and Yu, Z.: Eastward propagating planetary waves with periods of 1–5 days in the winter Antarctic stratosphere as revealed by MERRA and lidar, Journal of Geophysical Research: Atmospheres, 118, 9565-9578, https://doi.org/10.1002/jgrd.50717, 2013.

Lu, X., Wu, H., Chu, X., Oberheide, J., Mlynczak, M. G., and Russell Iii, J. M.: Quasi-Biennial Oscillation of Short-Period Planetary Waves and Polar Night Jet in Winter Antarctica Observed in SABER and MERRA-2 and Mechanism Study With a Quasi-Geostrophic Model, Geophysical Research Letters, 46, 13526-13534, https://doi.org/10.1029/2019GL084759, 2019.

Manney, G. L. and Randel, W. J.: Instability at the Winter Stratopause: A Mechanism for the 4-Day Wave, Journal of Atmospheric Sciences, 50, 3928-3938, 10.1175/1520-0469(1993)050<3928:IATWSA>2.0.CO;2, 1993.

Manney, G. L., Orsolini, Y. J., Pumphrey, H. C., and Roche, A. E.: The 4-Day Wave and Transport of UARS Tracers in the Austral Polar Vortex, Journal of the Atmospheric Sciences, 55, 3456-3470, https://doi.org/10.1175/1520-0469(1998)055<3456:TDWATO>2.0.CO;2, 1998.

Merzlyakov, E. G. and Pancheva, D. V.: The 1.5–5-day eastward waves in the upper stratosphere–mesosphere as observed by the Esrange meteor radar and the SABER instrument, Journal of Atmospheric and Solar-Terrestrial Physics, 69, 2102-2117, https://doi.org/10.1016/j.jastp.2007.07.002, 2007.

Molod, A., Takacs, L., Suarez, M., and Bacmeister, J.: Development of the GEOS-5 atmospheric general circulation model: evolution from MERRA to MERRA2, Geoscientific Model Development Discussions, 7, 10.5194/gmdd-7-7575-2014, 2014.

Molod, A., Takacs, L., Suarez, M., Bacmeister, J., Song, I. S., and Eichmann, A.: The GEOS-5 Atmospheric General Circulation Model: Mean Climate and Development from MERRA to Fortuna, 2012.

Pancheva, D. V., Mukhtarov, P. J., Mitchell, N. J., Fritts, D. C., Riggin, D. M., Takahashi, H., Batista, P. P., Clemesha, B. R., Gurubaran, S., and Ramkumar, G.: Planetary wave coupling (5–6-day waves) in the low-latitude atmosphere–ionosphere system, Journal of Atmospheric and Solar-Terrestrial Physics, 70, 101-122, https://doi.org/10.1016/j.jastp.2007.10.003, 2008.

Rhodes, C. T., Limpasuvan, V., and Orsolini, Y. J.: Eastward-Propagating Planetary Waves Prior to

https://doi.org/10.5194/egusphere-2024-3121
Preprint. Discussion started: 8 November 2024

the January 2009 Sudden Stratospheric Warming, Journal of Geophysical Research: Atmospheres, 126, e2020JD033696, https://doi.org/10.1029/2020JD033696, 2021.

Sandford, D. J., Schwartz, M. J., and Mitchell, N. J.: The wintertime two-day wave in the polar stratosphere, mesosphere and lower thermosphere, Atmos. Chem. Phys., 8, 749-755, 10.5194/acp-8-749-2008, 2008.

Tang, L. and Gu, S.-Y.: Interannual and Interhemispheric Comparisons of Q2DW Bimodal and Unimodal Structures During the 2003–2020 Summer Period, Journal of Geophysical Research: Space Physics, 128, e2023JA031412, https://doi.org/10.1029/2023JA031412, 2023.

Tang, L., Gu, S. Y., and Dou, X. K.: Eastward-propagating planetary waves in the polar middle atmosphere, Atmos. Chem. Phys., 21, 17495-17512, 10.5194/acp-21-17495-2021, 2021.

Tunbridge, V. M. and Mitchell, N. J.: The two-day wave in the Antarctic and Arctic mesosphere and lower thermosphere, Atmospheric Chemistry and Physics, 9, 6377-6388, DOI 10.5194/acp-9-6377-2009, 2009.

Ukhov, A., Mostamandi, S., da Silva, A., Flemming, J., Alshehri, Y., Shevchenko, I., and Stenchikov, G.: Assessment of natural and anthropogenic aerosol air pollution in the Middle East using MERRA-2, CAMS data assimilation products, and high-resolution WRF-Chem model simulations, Atmospheric Chemistry and Physics, 20, 9281-9310, 10.5194/acp-20-9281-2020, 2020.

Venne, D. E. and Stanford, J. L.: Observation of a 4–Day Temperature Wave in the Polar Winter Stratosphere, Journal of the Atmospheric Sciences, 36, 2016-2019, 10.1175/1520-0469(1979)036<2016:Ooatwi>2.0.Co;2, 1979.

Watanabe, S., Tomikawa, Y., Sato, K., Kawatani, Y., Miyazaki, K., and Takahashi, M.: Simulation of the eastward 4-day wave in the Antarctic winter mesosphere using a gravity wave resolving general circulation model, Journal of Geophysical Research: Atmospheres, 114, https://doi.org/10.1029/2008JD011636, 2009.

Yue, J., Liu, H. L., and Chang, L. C.: Numerical investigation of the quasi 2 day wave in the mesosphere and lower thermosphere, Journal of Geophysical Research Atmospheres, 117, 10.1029/2011JD016574, 2012.

Zamora, L. M., Kahn, R. A., Evangeliou, N., Groot Zwaaftink, C. D., and Huebert, K. B.: Comparisons between the distributions of dust and combustion aerosols in MERRA-2, FLEXPART, and CALIPSO and implications for deposition freezing over wintertime Siberia, Atmos. Chem. Phys., 22, 12269-12285, 10.5194/acp-22-12269-2022, 2022.

https://doi.org/10.5194/egusphere-2024-3121
Preprint. Discussion started: 8 November 2024

Table 1. Occurrence Date, Wave Period, and Peak Amplitude of the E1 polar planetary waves During the 2002–2022 Austral Winter Period

No.	Year	Day	Period(hr)	Amp(K)	No.	Year	Day	Period(hr)	Amp(K)
1	2002	154	92	6.1	55	2012	236	101	8.2
2	2002	184	84	5.0	56	2013	150	107	7.2
3	2002	202	72	11.1	57	2013	166	112	9.9
4	2003	160	102	4.3	58	2013	194	69	8.1
5	2003	174	88	7.9	59	2013	204	78	8.6
6	2003	214	74	13.7	60	2013	226	86	8.0
7	2004	158	164	9.1	61	2014	166	83	6.2
8	2004	168	104	9.4	62	2014	178	61	5.0
9	2004	196	88	9.6	63	2014	226	87	10.6
10	2004	216	87	11.6	64	2014	248	75	5.8
11	2005	142	83	5.5	65	2015	146	105	8.1
12	2005	154	107	4.8	66	2015	166	126	9.7
13	2005	162	105	7.4	67	2015	192	106	11.4
14	2005	204	67	10.5	68	2015	242	171	9.4
15	2005	218	73	13.3	69	2015	258	104	7.2
16	2006	142	94	6.7	70	2016	144	99	6.0
17	2006	194	109	8.4	71	2016	150	77	6.5
18	2006	208	160	11.5	72	2016	158	99	6.2
19	2006	226	84	10.9	73	2016	176	93	7.6
20	2006	240	118	8.9	74	2016	200	59	5.6
21	2006	254	85	11.2	75	2016	224	94	10.5
22	2007	160	117	6.7	76	2016	240	79	8.5
23	2007	186	87	8.3	77	2017	176	69	5.3
24	2007	200	65	5.0	78	2017	194	108	13.9
25	2007	224	75	9.6	79	2017	212	85	10.8
26	2008	146	86	4.8	80	2017	226	89	8.7
27	2008	168	101	5.7	81	2017	234	114	8.1
28	2008	186	107	6.8	82	2017	240	62	4.7
29	2008	200	106	6.6	83	2018	150	95	7.7
30	2008	210	125	9.5	84	2018	172	85	6.6
31	2008	218	82	6.5	85	2018	192	136	6.8
32	2008	236	94	6.7	86	2018	206	168	9.6
33	2009	142	99	10.9	87	2018	212	81	8.5
34	2009	170	121	5.0	88	2018	236	109	12.3
35	2009	186	78	7.7	89	2018	258	75	5.1
36	2009	220	119	9.6	90	2019	186	101	8.3
37	2009	230	81	4.9	91	2019	204	83	9.7
38	2009	246	84	9.0	92	2019	212	66	9.5

https://doi.org/10.5194/egusphere-2024-3121
Preprint. Discussion started: 8 November 2024

39	2010	142	118	6.6	93	2019	230	88	8.2
40	2010	158	76	4.0	94	2020	164	106	6.5
41	2010	174	113	12.9	95	2020	182	144	5.2
42	2010	218	102	5.5	96	2020	218	66	8.6
43	2010	238	97	5.3	97	2020	238	111	5.6
44	2011	146	92	5.6	98	2021	142	107	4.4
45	2011	170	132	8.5	99	2021	172	72	11.2
46	2011	190	109	12.2	100	2021	186	109	8.0
47	2011	214	91	11.4	101	2021	198	102	10.1
48	2011	238	83	10.1	102	2021	204	59	6.5
49	2011	258	88	6.5	103	2022	186	83	9.4
50	2012	160	117	8.1	104	2022	202	145	5.7
51	2012	182	95	12.8	105	2022	210	68	7.7
52	2012	190	53	5.7	106	2022	224	109	12.2
53	2012	196	85	7.5	107	2022	256	82	7.7
54	2012	208	79	5.5					

Table 2. Occurrence Date, Wave Period, and Peak Amplitude of the E2 polar planetary waves During the 2002–2022 Austral Winter Period

No.	Year	Day	Period(hr)	Amp(K)	No.	Year	Day	Period(hr)	Amp(K)
1	2002	186	32	6.2	51	2012	238	52	4.9
2	2002	198	35	3.2	52	2013	164	37	6.8
3	2002	208	39	5.1	53	2013	194	45	5.7
4	2003	142	42	4.5	54	2013	204	35	5.5
5	2003	162	44	5.5	55	2013	228	43	9.5
6	2003	182	40	8.1	56	2014	150	51	5.7
7	2003	208	42	6.9	57	2014	178	46	4.4
8	2003	228	38	7.5	58	2014	186	34	6.8
9	2003	250	47	4.3	59	2014	222	36	9.5
10	2004	164	41	7.5	60	2015	158	41	3.8
11	2004	192	45	6.6	61	2015	174	44	8.9
12	2004	206	31	6.0	62	2015	210	43	7.4
13	2004	254	56	5.2	63	2015	218	42	9.2
14	2005	160	46	6.1	64	2015	248	48	6.7
15	2005	178	39	5.8	65	2016	152	39	7.4
16	2005	192	37	6.2	66	2016	180	36	5.9
17	2005	226	39	5.1	67	2016	204	39	7.4
18	2005	256	47	3.7	68	2016	232	36	4.1
19	2006	148	52	5.1	69	2016	244	43	3.4
20	2006	176	42	4.3	70	2017	142	47	5.3
21	2006	188	44	6.4	71	2017	162	43	8.2
22	2006	220	46	4.9	72	2017	196	40	5.5

https://doi.org/10.5194/egusphere-2024-3121
Preprint. Discussion started: 8 November 2024

23	2006	246	40	8.5	73	2017	214	30	4.1
24	2007	162	43	6.3	74	2017	238	30	3.6
25	2007	174	44	11.5	75	2017	246	43	2.5
26	2007	190	43	7.6	76	2018	156	46	3.3
27	2007	210	43	9.0	77	2018	180	51	4.9
28	2007	244	40	9.2	78	2018	198	51	4.1
29	2008	150	43	4.1	79	2018	204	38	6.1
30	2008	172	39	6.8	80	2018	240	41	7.2
31	2008	192	41	7.9	81	2019	144	45	5.1
32	2008	224	41	10.3	82	2019	174	39	6.6
33	2008	246	46	5.9	83	2019	208	35	7.7
34	2009	168	43	9.0	84	2019	220	44	6.9
35	2009	184	44	5.6	85	2020	160	43	7.3
36	2009	224	48	9.5	86	2020	178	44	8.0
37	2010	160	47	6.7	87	2020	202	37	6.9
38	2010	174	39	4.9	88	2020	220	37	11.4
39	2010	190	39	6.4	89	2020	236	51	6.7
40	2010	216	41	3.4	90	2021	148	47	5.2
41	2010	232	38	3.9	91	2021	158	42	7.2
42	2010	248	45	3.6	92	2021	176	42	4.5
43	2011	160	44	8.7	93	2021	204	46	6.6
44	2011	178	45	9.4	94	2022	142	49	4.9
45	2011	208	40	6.5	95	2022	166	49	7.0
46	2011	240	46	7.7	96	2022	192	41	10.2
47	2011	256	58	5.1	97	2022	202	44	7.3
48	2012	150	57	4.6	98	2022	230	42	6.4
49	2012	176	58	7.4	99	2022	240	54	8.0
50	2012	210	39	7.0					

Table 3. Occurrence Date, Wave Period, and Peak Amplitude of the E3 polar planetary waves During the 2002–2022 Austral Winter Period

No.	Year	Day	Period(hr)	Amp(K)	No.	Year	Day	Period(hr)	Amp(K)
1	2002	154	27	4.5	38	2013	190	22	4.3
2	2002	186	23	4.4	39	2013	204	36	3.3
3	2003	160	28	4.4	40	2013	226	24	3.0
4	2003	174	30	7.5	41	2014	148	29	6.8
5	2003	196	25	7.0	42	2014	176	26	5.5
6	2003	212	24	5.2	43	2014	190	26	6.5
7	2004	156	22	1.9	44	2014	218	23	3.9
8	2004	184	27	7.1	45	2015	178	27	6.4
9	2004	252	35	3.4	46	2015	202	27	5.5
10	2005	160	32	4.3	47	2015	230	30	6.2

https://doi.org/10.5194/egusphere-2024-3121
Preprint. Discussion started: 8 November 2024

11	2005	186	26	7.7	48	2015	258	31	2.3
12	2005	228	26	3.6	49	2016	146	29	5.3
13	2006	150	31	6.3	50	2016	178	24	7.8
14	2006	204	21	2.6	51	2017	158	25	3.2
15	2006	242	26	4.9	52	2017	172	24	5.1
16	2006	258	29	2.3	53	2017	190	27	6.7
17	2007	156	31	5.3	54	2017	246	24	3.4
18	2007	176	31	7.9	55	2018	150	35	5.3
19	2007	238	27	2.7	56	2018	166	36	5.1
20	2008	158	28	4.7	57	2018	196	29	3.9
21	2008	180	27	9.0	58	2018	210	29	5.0
22	2008	214	27	4.1	59	2018	240	29	3.9
23	2008	238	30	5.8	60	2018	260	32	3.0
24	2009	182	29	7.0	61	2019	154	29	5.7
25	2009	206	30	5.9	62	2019	214	42	3.3
26	2009	236	24	4.0	63	2020	200	24	2.6
27	2009	260	38	2.2	64	2020	220	24	2.9
28	2010	158	29	4.4	65	2021	150	30	3.7
29	2010	186	27	5.7	66	2021	166	29	6.6
30	2010	224	29	5.3	67	2021	186	35	5.2
31	2010	244	28	4.1	68	2021	202	27	4.9
32	2011	170	29	7.2	69	2022	142	31	3.8
33	2011	188	30	5.0	70	2022	160	30	3.8
34	2011	238	29	7.0	71	2022	176	31	6.7
35	2012	146	26	2.9	72	2022	196	29	3.2
36	2012	178	30	4.7	73	2022	212	28	4.5
37	2013	164	26	5.5	74	2022	234	30	3.7

Table 4. Occurrence Date, Wave Period, and Peak Amplitude of the E4 polar planetary waves During the 2002–2022 Austral Winter Period

No.	Year	Day	Period(hr)	Amp(K)	No.	Year	Day	Period(hr)	Amp(K)
1	2002	154	18	1.1	36	2012	210	18	2.0
2	2002	192	21	1.3	37	2013	156	21	2.7
3	2002	224	27	1.6	38	2013	172	19	3.2
4	2003	142	23	1.8	39	2013	190	18	2.9
5	2003	170	24	4.5	40	2014	166	23	3.9
6	2003	194	21	4.1	41	2015	142	27	5.7
7	2004	166	22	4.4	42	2015	164	23	5.1
8	2004	186	21	2.0	43	2015	196	21	5.7
9	2005	150	26	3.6	44	2015	210	20	4.9
10	2005	164	24	3.7	45	2015	232	23	4.2
11	2005	194	20	2.8	46	2016	148	23	2.4

https://doi.org/10.5194/egusphere-2024-3121
Preprint. Discussion started: 8 November 2024

12	2006	148	23	4.0	47	2016	158	20	4.0
13	2006	170	21	2.9	48	2016	192	22	3.3
14	2006	202	22	4.3	49	2017	164	23	6.0
15	2006	214	23	3.8	50	2017	194	19	3.5
16	2006	254	25	1.8	51	2018	150	25	2.9
17	2007	206	21	2.7	52	2018	170	24	4.6
18	2008	142	21	3.2	53	2018	186	27	4.1
19	2008	168	18	4.6	54	2018	194	20	2.2
20	2008	218	23	3.6	55	2018	208	23	5.5
21	2008	230	22	6.3	56	2019	144	25	3.0
22	2009	142	26	3.7	57	2019	162	23	3.7
23	2009	154	24	2.8	58	2019	180	21	3.1
24	2009	184	21	4.6	59	2020	178	20	2.8
25	2009	202	21	3.3	60	2020	230	23	2.2
26	2009	226	23	2.8	61	2021	142	22	2.4
27	2010	160	26	5.1	62	2021	160	22	4.9
28	2010	176	21	2.5	63	2021	182	24	3.5
29	2010	240	24	3.9	64	2021	208	17	4.4
30	2011	152	25	4.0	65	2022	156	22	4.4
31	2011	190	22	3.6	66	2022	172	22	4.9
32	2011	224	19	3.5	67	2022	200	22	4.1
33	2011	248	26	3.1	68	2022	206	20	3.9
34	2012	164	23	5.6	69	2022	222	22	3.6
35	2012	180	25	5.9					

https://doi.org/10.5194/egusphere-2024-3121
Preprint. Discussion started: 8 November 2024

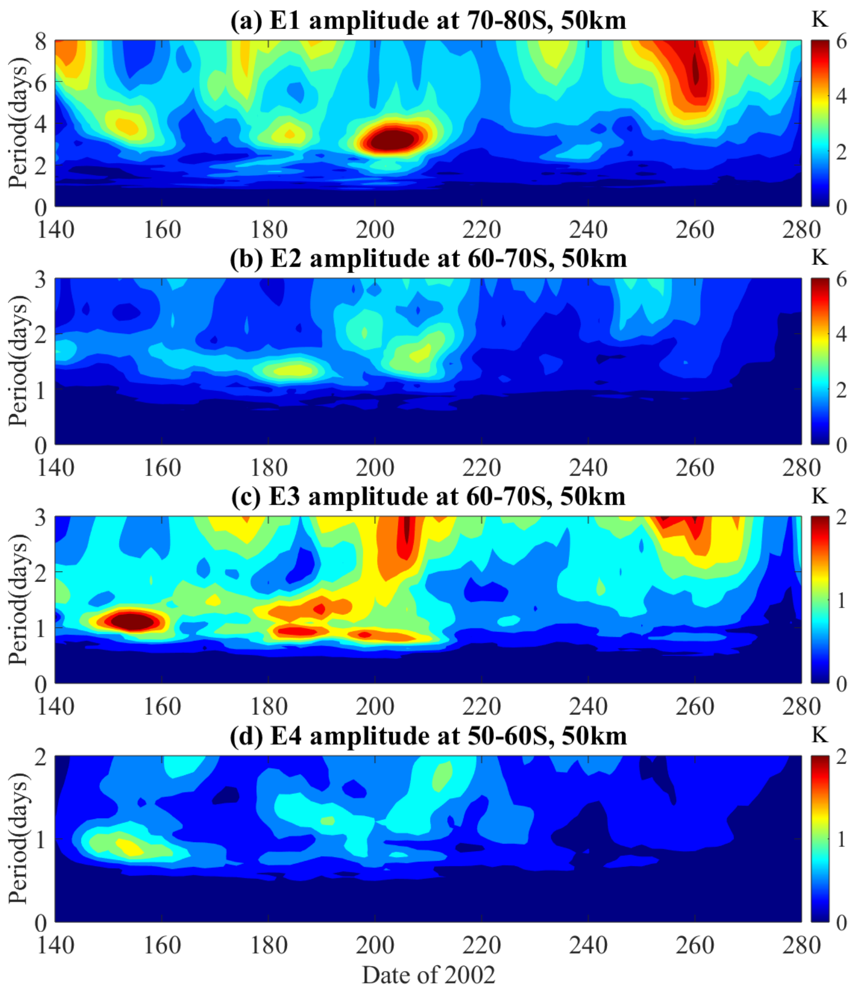

Figure 1. The temporal variations in (a) E1, (b) E2, (c) E3, and (d) E4 during the 2002 austral winter period are depicted. The event dates indicate day +9, +5, +3, and +3 for E1, E2, E3, and E4, respectively.

https://doi.org/10.5194/egusphere-2024-3121
Preprint. Discussion started: 8 November 2024

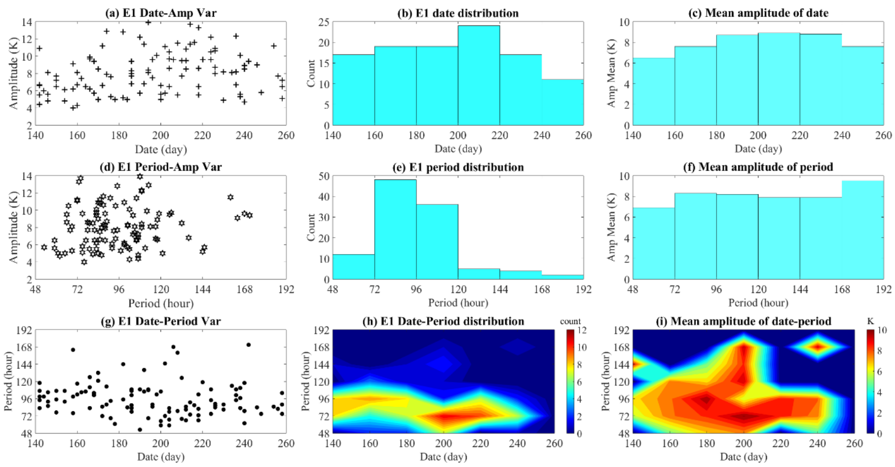

Figure 2. The dispersion of E1 (a) date-amplitude, (d) period-amplitude, and (g) date-period variations during the austral winter period from 2002 to 2022. Statistical findings for the occurrence dates (b, e, and h) and mean amplitude (c, f, and i) of E1.

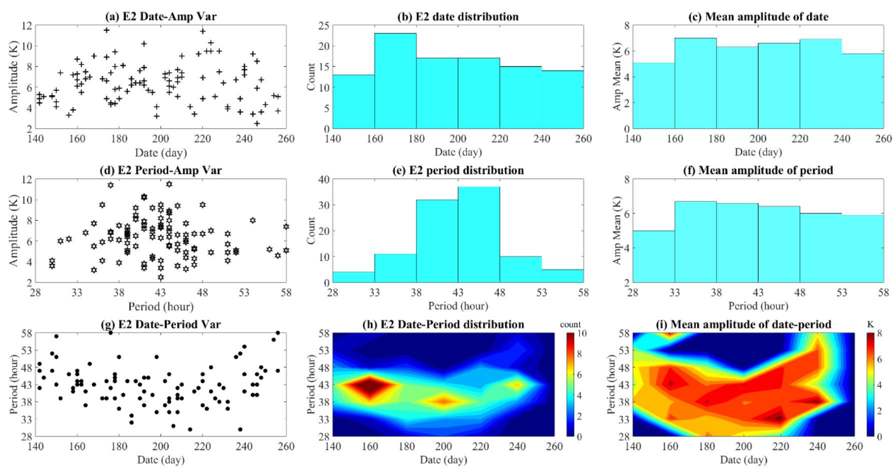

Figure 3. Same as Figure 2 but for E2.

https://doi.org/10.5194/egusphere-2024-3121
Preprint. Discussion started: 8 November 2024

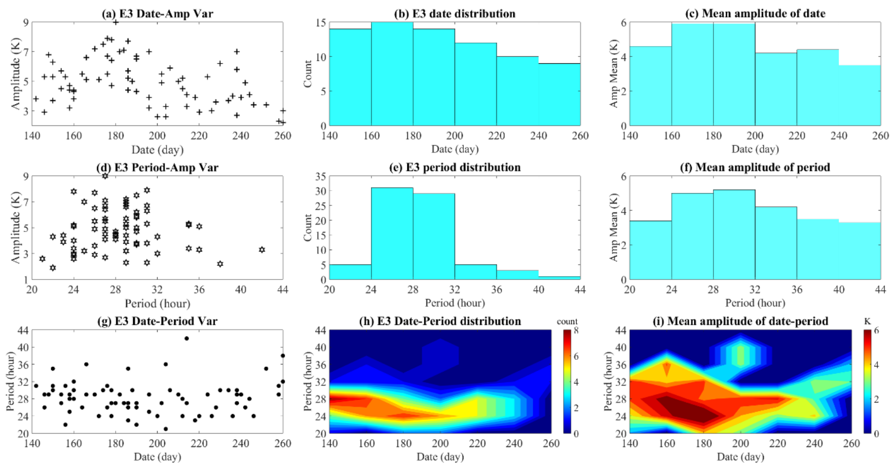

Figure 4. Same as Figure 3 but for E3.

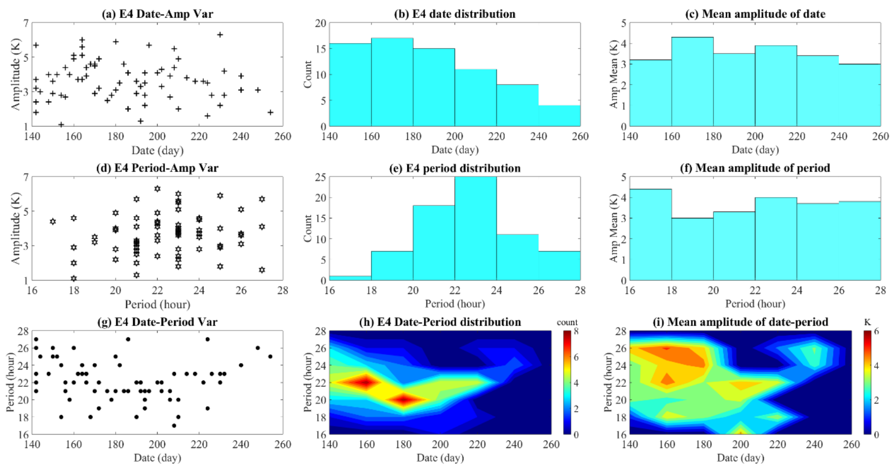

Figure 5. Same as Figure 4 but for E4.

https://doi.org/10.5194/egusphere-2024-3121
Preprint. Discussion started: 8 November 2024

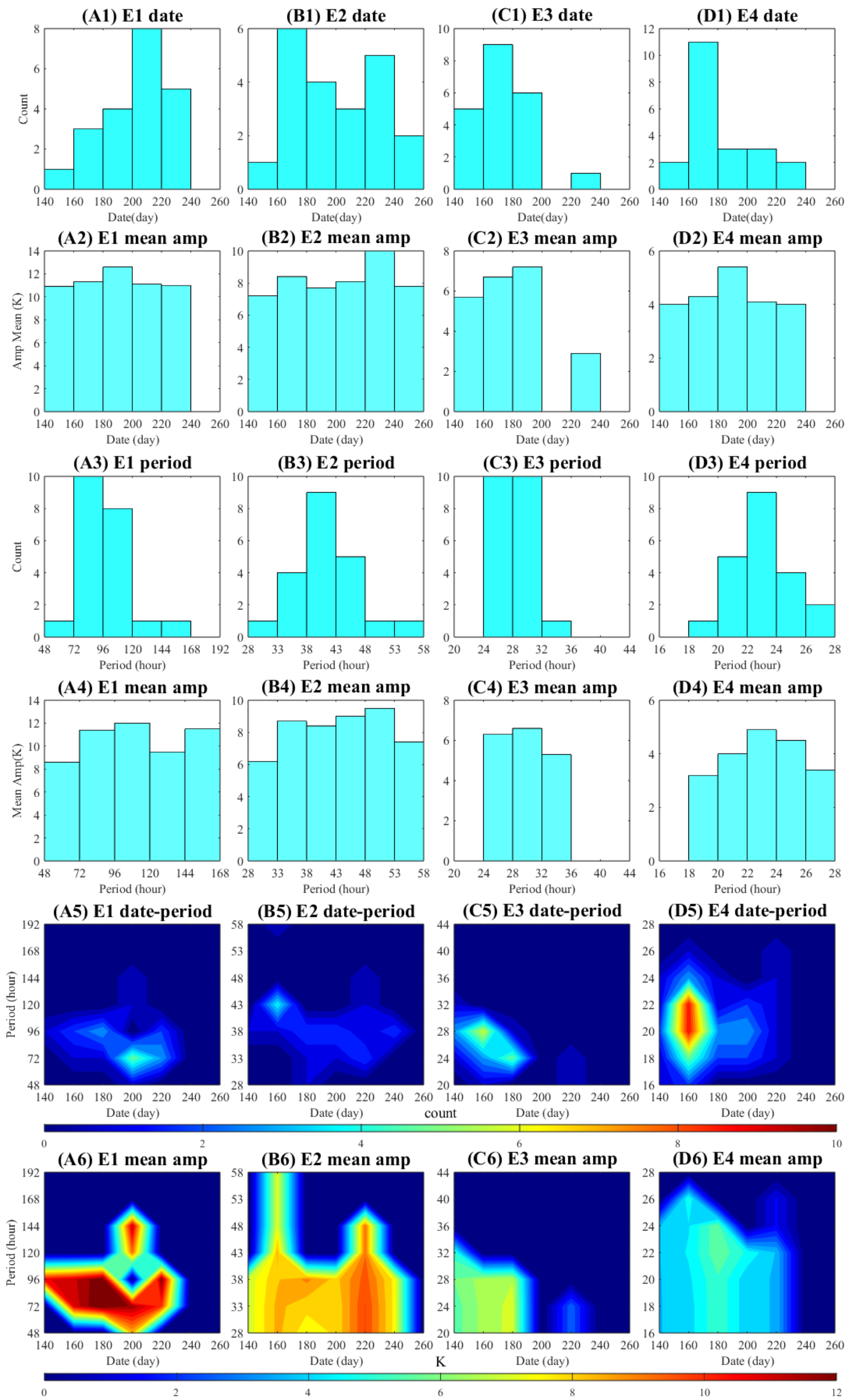

1092

https://doi.org/10.5194/egusphere-2024-3121
Preprint. Discussion started: 8 November 2024

Figure 6. Statistical results of the strongest austral winter E1 (Column 1), E2 (Column 2), E3 (Column 3), and E4 (Column 4) events occurring between 2002 and 2022 are presented.

https://doi.org/10.5194/egusphere-2024-3121
Preprint. Discussion started: 8 November 2024

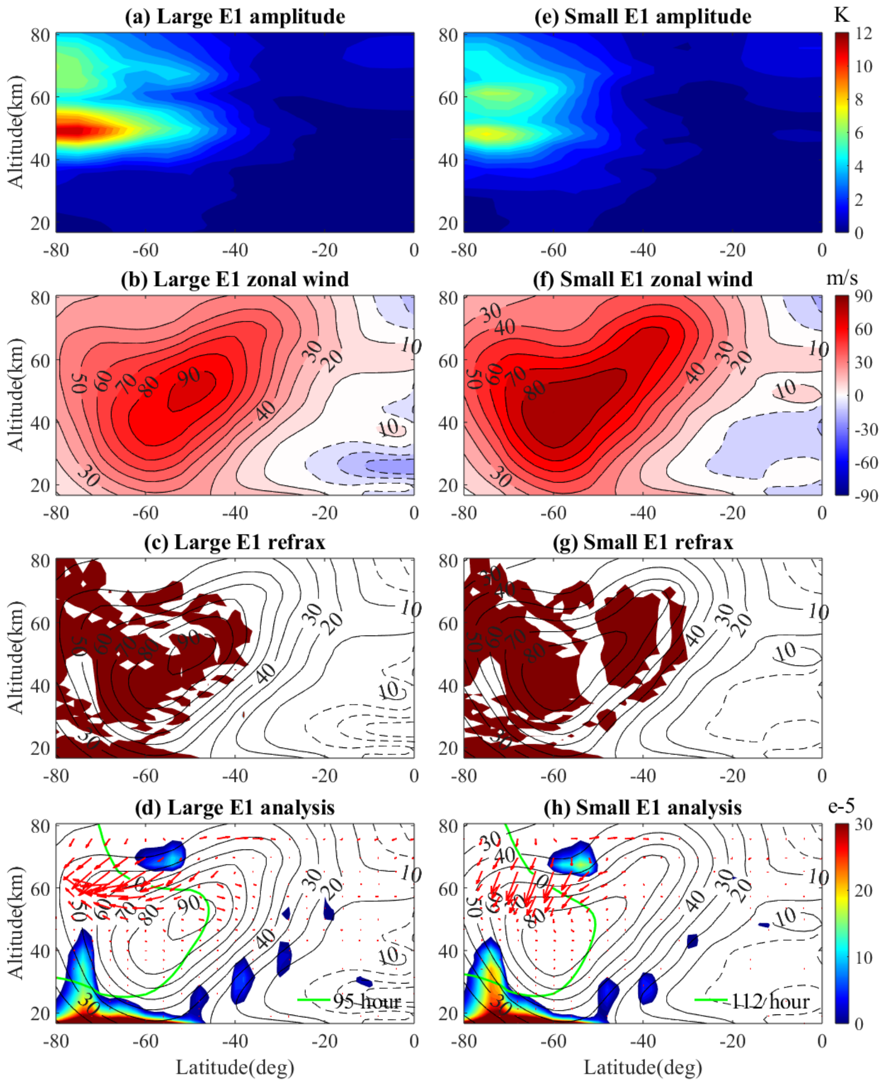

1096

1097 **Figure 7.** The mean spatial structures of the E1 large and small amplitude events during the 2002 to 2022 are characterized by variations in temperature, zonal wind, positive refractive index and diagnostic analysis. The shaded regions in the diagnostic analysis indicate areas of instability, while the red arrows represent EP flux and the green line denotes the critical layer. The brown area signifies a positive refractive index.

https://doi.org/10.5194/egusphere-2024-3121
Preprint. Discussion started: 8 November 2024

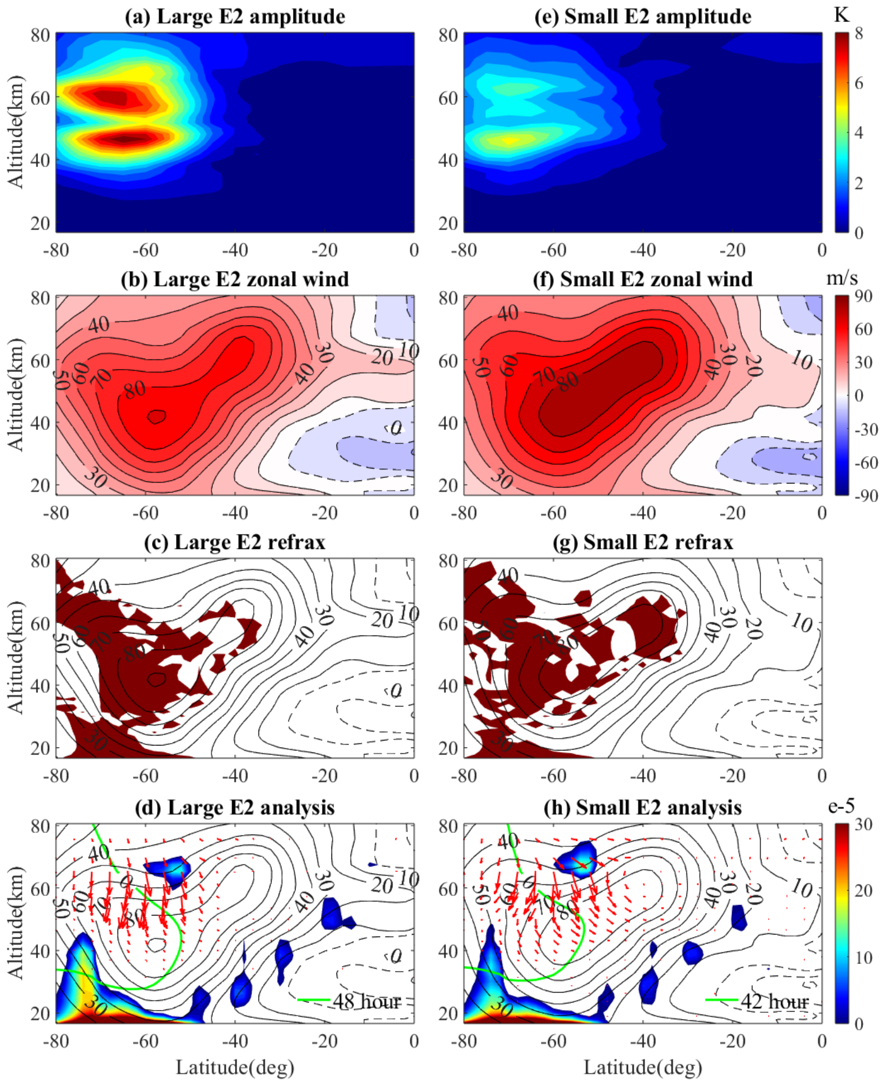

Figure 8. Same as Figure 7 but for E2.

https://doi.org/10.5194/egusphere-2024-3121
Preprint. Discussion started: 8 November 2024

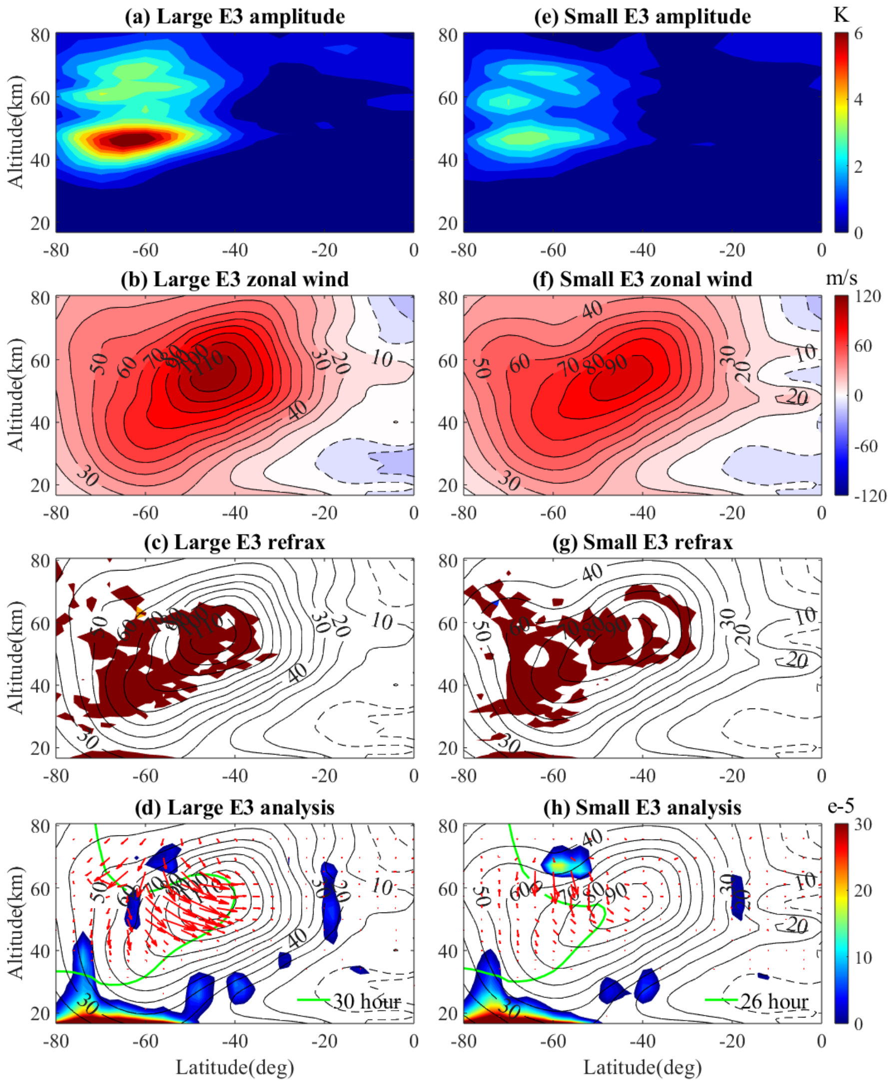

1105

1106 **Figure 9.** Same as Figure 8 but for E3.

https://doi.org/10.5194/egusphere-2024-3121
Preprint. Discussion started: 8 November 2024

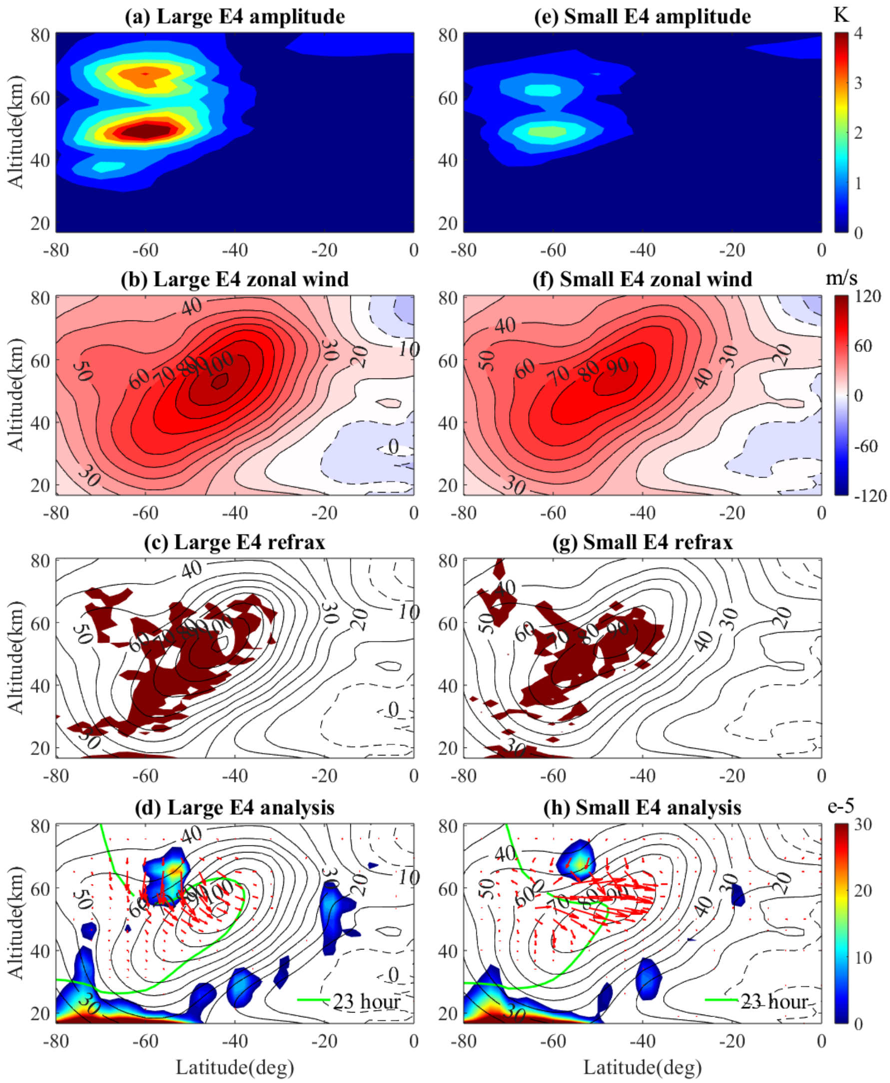

1108 **Figure 10.** Same as Figure 9 but for E4.

https://doi.org/10.5194/egusphere-2024-3121
Preprint. Discussion started: 8 November 2024

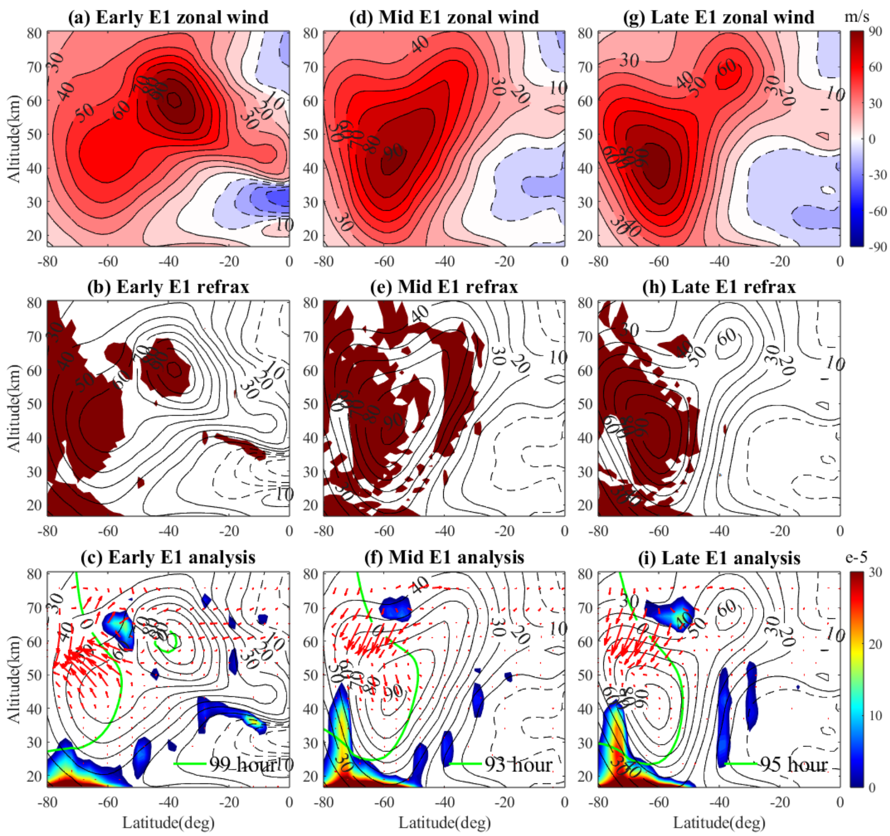

Figure 11. The mean spatial structure of E1 early, middle, and late events from 2002 to 2022 is characterized by temperature, zonal wind, positive refractive index, and diagnostic analysis (early: 140-160 days, early: 200-220 days, early: 220-240 days).

https://doi.org/10.5194/egusphere-2024-3121
Preprint. Discussion started: 8 November 2024

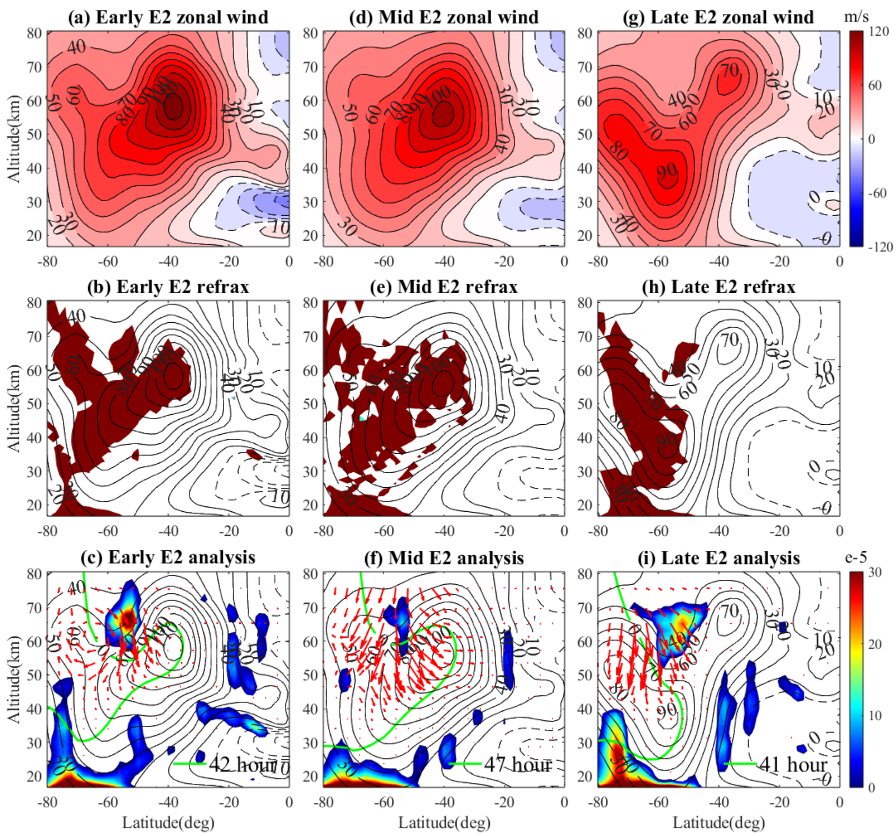

Figure 12. Same as Figure 11 but for E2 (early: 140-160 days, early: 160-180 days, early: 240-260 days).

https://doi.org/10.5194/egusphere-2024-3121
Preprint. Discussion started: 8 November 2024

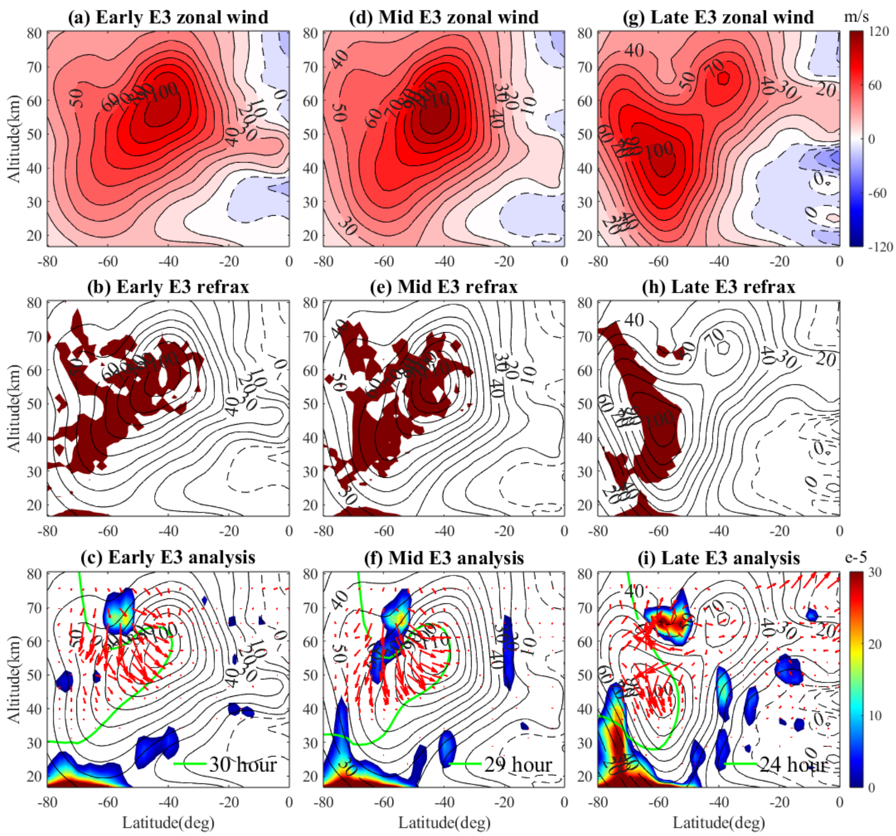

Figure 13. Same as Figure 12 but for E3 (early: 140-160 days, early: 160-180 days, early: 220-240 days).

https://doi.org/10.5194/egusphere-2024-3121
Preprint. Discussion started: 8 November 2024

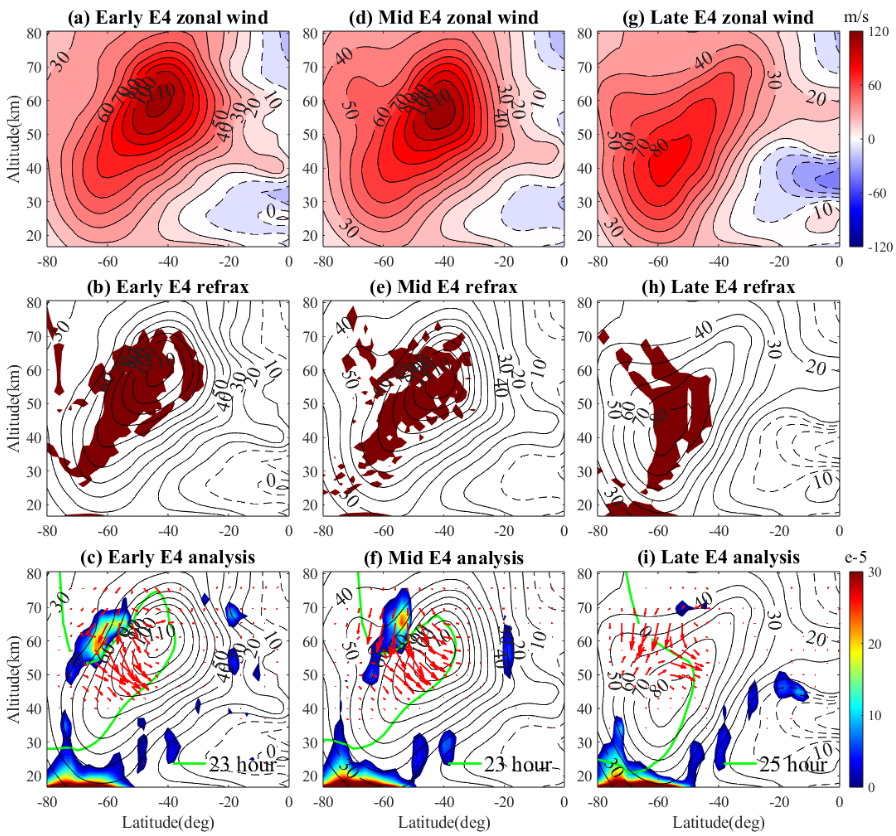

Figure 14. Same as Figure 13 but for E4 (early: 140-160 days, early: 160-180 days, early: 220-240 days).

https://doi.org/10.5194/egusphere-2024-3121
Preprint. Discussion started: 8 November 2024

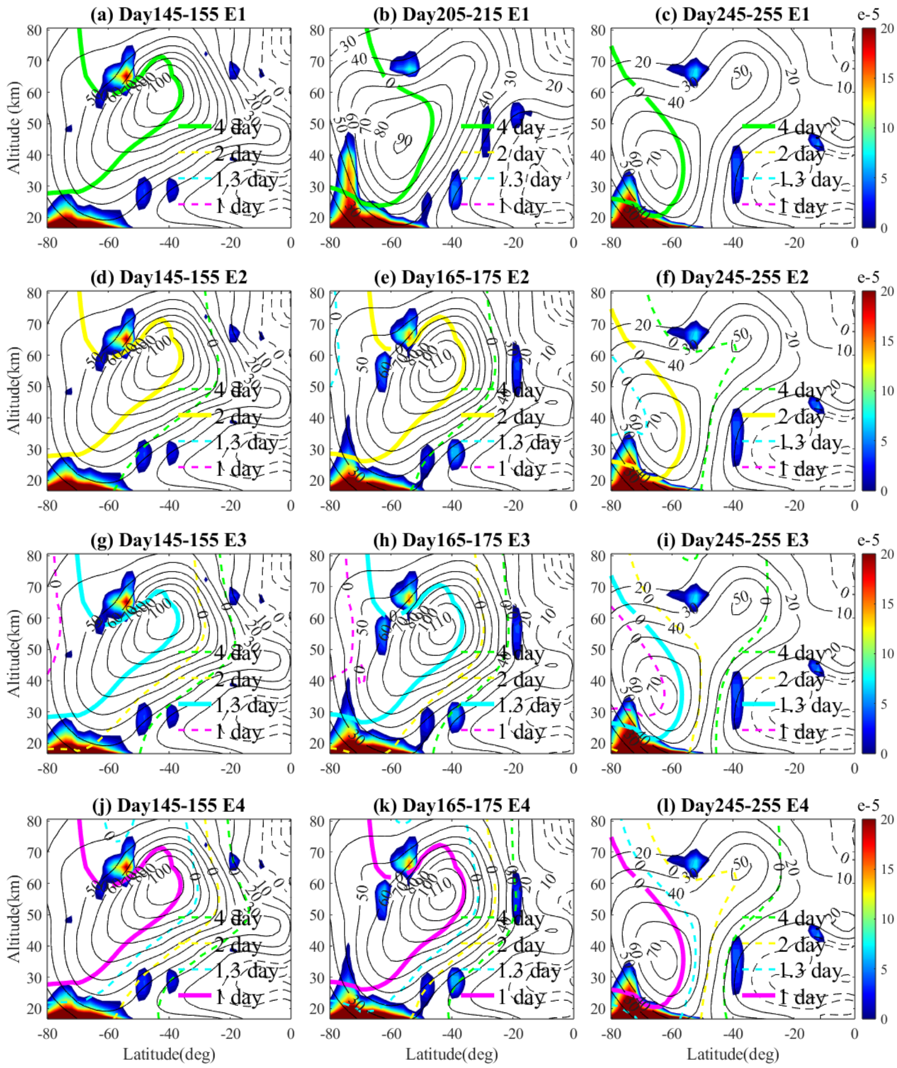

Figure 15. The green, yellow, cyan, and magenta lines represent critical layers corresponding to the 4-day, 2-day, 1.3-day, and 1-day wave periods for planetary waves E1, E2, E3, and E4 during days 145–155 (a, d, g, and j), days 205–215 (b), days 165–175 (e, h, and k), and days 245–255 (c, f, i, and l) from 2002 to 2022.

https://doi.org/10.5194/egusphere-2024-3121
Preprint. Discussion started: 8 November 2024

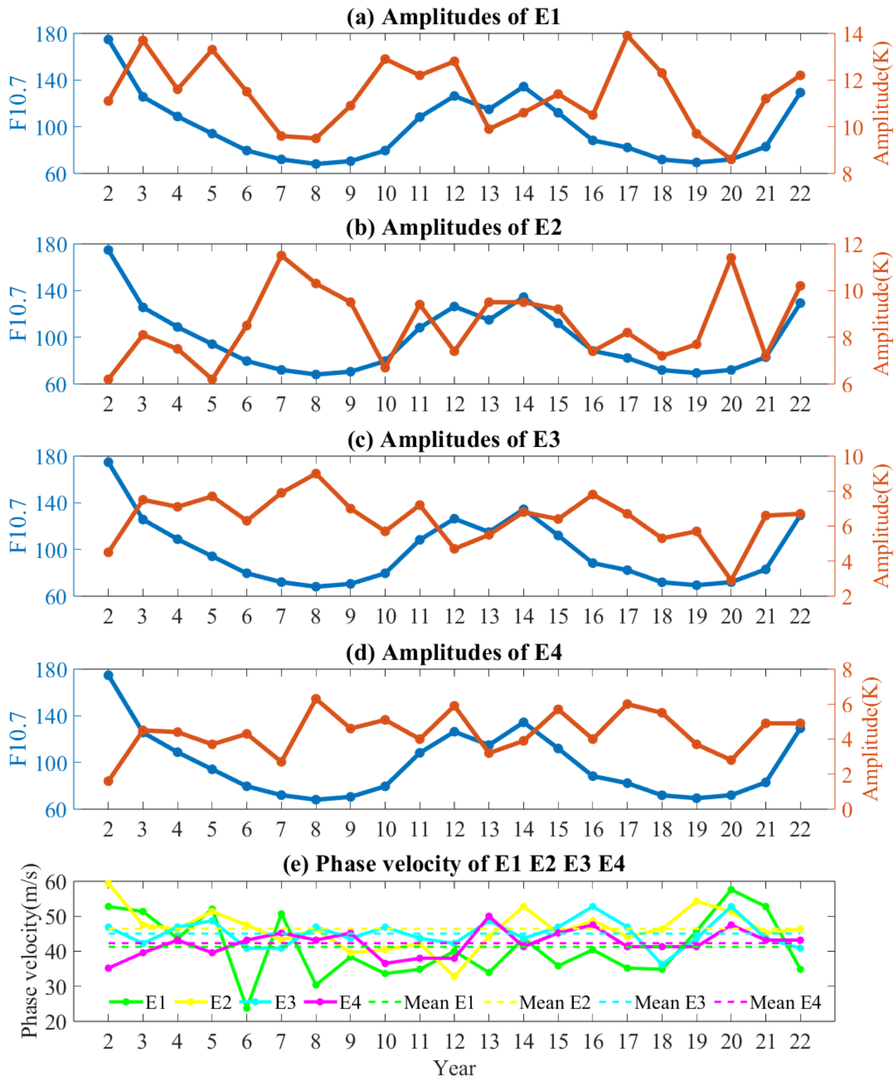

Figure 16. The strongest amplitudes of E1 (a), E2 (b), E3 (c), and E4 (d) during 2002 to 2022 are depicted. The blue line represents the mean 10.7 cm solar flux during the austral winter, while the orange line illustrates the strongest amplitude of E1, E2, E3, and E4. Description of phase velocities (e) for the strongest events (E1, E2, E3, and E4).